PNNL-16538

Pacific Northwest
National Laboratory
Operated by Battelle for the
U.S. Department of Energy

T Tank Farm Interim Surface Barrier Demonstration – Vadose Zone Monitoring Plan

Z. F. Zhang
J. M. Keller
C. E. Strickland

April 2007

Prepared for the U.S. Department of Energy
under Contract DE-AC05-76RL01830

DISCLAIMER

PACIFIC NORTHWEST NATIONAL LABORATORY
operated by

BATTELLE
for the
UNITED STATES DEPARTMENT OF ENERGY
under Contract DE-AC05-76RL01830

Printed in the United States of America

Available to DOE and DOE contractors from the
Office of Scientific and Technical Information,
P.O. Box 62, Oak Ridge, TN 37831-0062;
ph: (865) 576-8401
fax: (865) 576 5728
email: reports@adonis.osti.gov

PNNL-16538

T Tank Farm Interim Surface Barrier Demonstration – Vadose Zone Monitoring Plan

Z. F. Zhang
J. M. Keller
C. E. Strickland

April 2007

Prepared for the U.S. Department of Energy
under Contract DE-AC05-76RL01830

Pacific Northwest National Laboratory
Richland, Washington 99352

Summary

The Hanford Site has 149 underground single-shell tanks that store hazardous radioactive waste. Many of these tanks and their associated infrastructure (e.g., pipelines, diversion boxes) have leaked. Some of the leaked waste has entered the groundwater. The largest known leak occurred from the T-106 Tank in 1973. Many of the contaminants from that leak still reside within the vadose zone beneath the T Tank Farm. CH2M Hill Hanford Group, Inc. seeks to minimize movement of this residual contaminant plume by placing an interim barrier on the surface. Such a barrier is expected to prevent infiltrating water from reaching the plume and moving it further. A plan has been prepared to monitor and determine the effectiveness of the interim surface barrier. Soil-water content (θ) and water pressure (ψ) will be monitored using off-the-shelf equipment that can be installed by the hydraulic hammer technique. Two instrument nests were installed in fiscal year (FY) 2006. Each instrument nest contains a neutron probe access tube, a capacitance probe (to measure θ), four heat-dissipation units (to measure ψ), and a drain gauge to measure soil-water flux. A meteorological station has been installed outside of the fence. Two additional instrument nests are planned to be installed beneath the proposed barrier in FY 2007.

Acronyms

ARHCO	Atlantic-Richfield Hanford Company
CCU	Cold Creek Unit
CHG	CH2M Hill Hanford Group, Inc.
CSI	Campbell Scientific, Inc.
DOE	Department of Energy
FY	Fiscal year
HDU	Heat-dissipation unit
HMS	Hanford Meteorological Station
IAEA	International Atomic Energy Agency
ID	Inside Diameter
OD	Outside Diameter
PMP	Project Management Plan
PNNL	Pacific Northwest National Laboratory
PVC	Polyvinyl chloride
QAP	Quality Assurance Plan
SST	Single-shell tank
STOMP	Subsurface Transport Over Multiple Phases
WIDS	Waste Information Data System
WMA	Waste Management Area

Table of Contents

Figures

Tables

1.0 Introduction

The Hanford Site in southeastern Washington State has 149 underground single-shell tanks (SSTs) that store hazardous radioactive waste. Many of these tanks and their associated infrastructure (e.g., pipelines, diversion boxes) have leaked. Some of the leaked waste has entered the groundwater. The largest known leak occurred from the T-106 Tank in 1973. Many of the contaminants from that leak still reside within the vadose zone beneath the T Tank Farm. CH2M Hill Hanford Group, Inc. (CHG) seeks to minimize movement of this residual contaminant plume by placing an interim barrier on the surface. This monitoring plan is prepared to guide the monitoring program and will replace a previous prepared design plan.

1.1 T Tank Farm and Tank T-106 Leak

According to Myers (2005), the T tank farm was built from 1943 to 1944. The T tank farm contains 12 SSTs with a diameter of 23 m (75 ft) and a capacity of 2,006,050 L (530,000 gal), four SSTs with a diameter of 6.1 m (20 ft) and a capacity of 208,175 L (55,000 gal), waste-transfer lines, leak-detection systems, and tank ancillary equipment. The soil cover from the apex of the tank domes to ground surface is approximately 2.2 m (7.3 ft). All the tanks have a dish-shaped bottom. Figure 1.1 shows the waste management area (WMA) of the T tank farm and surrounding facilities.

In general, the vadose zone in the T tank farm consists of a portion of the thick, relatively coarse-grained sediments of the middle Ringold Formation (R_{wi}) overlain by the finer grained sediments of the upper Ringold Formation (R_{tf}) and the Plio-Pleistocene unit (also called the Cold Creek Unit, CCU), overlain by the coarser grained sands and gravels of the Hanford formation (H), which are exposed at the surface. The upper 12 m (40 ft) of the Hanford formation was locally excavated and backfilled with gravelly sand during installation of the SSTs.

According to Hanford's Waste Information Data System (WIDS), an accidental leak from Tank T-106 occurred in 1973, and the details and chronology of the leak are well documented (ARHCO 1973; Routson et al. 1979). The leak was suspected to have started on April 20, 1973, during a routine filling operation. The leak stopped on June 10, 1973, when the free liquid contents of the tank were removed. The total duration of the leak was estimated to be 51 days. Approximately 435,000 L (115,000 gal) of fluid leaked from Tank T-106. The fluid contained cesium-137, strontium-90, plutonium, and various fission products, including technetium-99. It is likely that the leak occurred in the southeast quadrant of the tank near the bottom of the tank side.

CHG has proposed to use an interim surface barrier over Tank T-106 and the surrounding area in the T-tank farm to prevent or reduce infiltration of meteoric water entering into the subsurface to reduce the rate of the downward movement of leaked contaminants.

1.2 Surface Barrier and Monitoring

CH2M HILL Hanford Group has proposed to use felt with a polyurea coating as an interim barrier over the part of the T Tank Farm in Hanford. It is expected that the interim barrier will prevent the meteoric water from entering into soil and consequently will reduce the rate of downward movement of flow and dissolving contaminants. At shallower depths, there will be no water supply from above to replace the

draining water, and hence, it will dry up more quickly. At larger depths, soil will keep receiving drainage from the soil above for some time and will drain relatively more slowly. Therefore, it may take a very long time (e.g., years) for drainage rates deep in the profile (e.g., > 10 m) to reduce significantly. As the soil below the surface barrier becomes drier, the soil in the uncovered region near the vertical plane directly beneath the barrier edge will also be drier than would be the case if there would be no surface barrier.

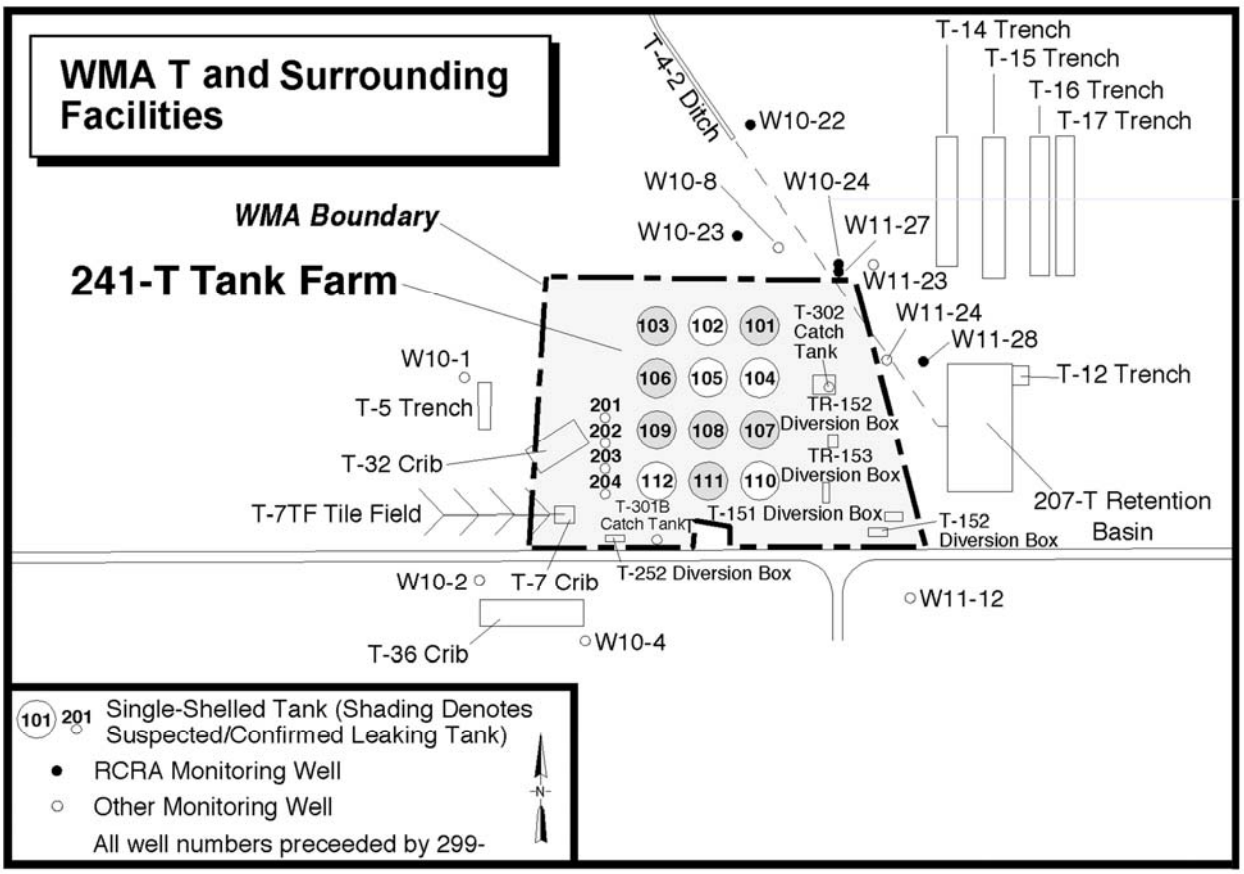

Figure 1.1. Waste Management Area of the T Tank Farm and Surrounding Facilities (from Myers 2005)

In fiscal year (FY) 2006, two instrument nests were installed by the hydraulic hammer technique outside of the proposed surface barrier. Soil-water content (θ), water pressure (ψ), and temperature (T) are monitored using neutron probes, capacitance probes, and heat-dissipation units (HDUs). In FY 2007, two additional instrument nests, both inside the proposed surface barrier, will be installed. Each instrument nest will contain a neutron access tube and a capacitance probe (to measure θ), and four HDUs (to measure ψ and T).

1.3 Objectives and Scope

Subsurface monitoring is integral to achieving acceptance of covers. The subsurface water conditions will be monitored to verify impacts of the T-106 interim barrier on the soil-moisture regime.

This monitoring plan updates the previous design plan and provides additional technical details for monitoring the soil-water regime and evaluating the impacts of the interim surface barrier on sub-surface moisture conditions. After a brief introduction of the background information in Chapter 1, Chapter 2 summarizes the numerical simulation results, which were used as guidance for designing the monitoring system. Chapter 3 presents the principles of relevant measurement methods as guidance for equipment calibration. In Chapter 4, equipment calibration or verification procedures and results are presented. Chapter 5 summarizes the installation of the two existing instrument nests and the plan for installing two additional nests. Chapter 6 presents the schedule of data collection, data validation and analysis, contingencies given instrument failure, and data reporting. Chapter 7 provides a declaration about the quality assurance plan to verify the quality of the work.

2.0 Numerical Analysis

This section presents numerical simulation results of water flow after placing an interim surface barrier over a portion of the T tank farm. The Subsurface Transport Over Multiple Phases (STOMP) numerical simulator (White and Oostrom 2004) was used to predict the movement of vadose-zone water in response to placement of an interim surface barrier on July 1, 2007.

The interim surface barrier is expected to be an impermeable layer and will be sloped so that excess water is drained outside the T Farm. For this analysis, it is assumed that all excess water is successfully removed such that none infiltrates at the barrier edge.

The simulation was conducted for 50 years after placing the interim surface barrier. Water contents, pressure heads, and fluxes at specific locations were compared and contrasted to highlight changes caused by barrier placement. The results were used to guide sensor selection and placement (explained more fully in Section 3.0). Some gas-phase and temperature effects may be caused by the interim surface barrier, but these processes were considered secondary to the water-flow solution and were not simulated in this exercise. The following sections describe the geology and hydraulic properties, domain, initial and boundary conditions, and the simulation results.

2.1 Geology and Hydraulic Properties

The borehole C4104 drilled near T-106 showed the geology as six main layers whose depths and soil types are given in Table 2.1 (Serne et al. 2004). The hydraulic parameters for each of the geological formations were from Khaleel et al. (2004) and are listed in Table 2.2.

2.2 Simulation Domain, Initial and Boundary Conditions

The three-dimensional physical domain was discretized with 74 nodes in both the east-west (x) and north-south (y) directions and 55 nodes in the vertical (z) direction. Horizontal node spacing was uniformly 2 m; vertical spacing was uniformly 1 m. The total domain size was 148 m in the x and y directions and 55 m in the z direction. The origin of the simulation domain in the Hanford coordinate system was (x_0, y_0) = (566710, 136650) m. The domain includes the 12 large tanks (T-101 through T-112) but not other infrastructures (e.g., the 200 series tanks and trenches). The nodes representing each tank were treated as inactive and did not interact with the changing water conditions in the vadose zone.

Table 2.1. The Geological Formations of the 241-T Farm

Geology	Soil	Depth (m)	Depth (ft)
1. Backfill	Gravelly Sand	0–12.2	0–40
2. H1 Sand	Sand	12.2–24.4	40–80
3. H2 Sand	Silty Sand	24.4–28.3	80–93
4. Cold Creek Unit	Silty Sand	28.3–32.9	93–108
5. Upper Ringold Sand	Sand	32.9–36.9	108–121
6. Ringold Unit E	Sandy Gravel	36.9–55.0	121–180

Table 2.2. The Composite Hydraulic Parameters for Soils at Hanford's T Tank Farm (data from Khaleel et al. 2004)

Parameters	Sandy Gravel/ Gravelly Sand	Sand	Silty Sand
θ_s (m^3m^{-3})	0.138	0.382	0.435
θ_r (m^3m^{-3})	0.010	0.044	0.067
α (m^{-1})	0.021	0.012	0.0085
n (-)	1.374	1.616	1.851
K_s (m s^{-1})	5.600×10^{-4}	9.880×10^{-5}	2.400×10^{-4}
L (-)	0.5	0.5	0.5
θ_s: saturated water content; θ_r: residual water content; α: van Genuchten (1980) parameter related to soil capillarity; n: a parameter related to soil particle size distribution; K_s: saturated hydraulic conductivity; and L: the flow path connectivity-tortuosity coefficient.			

The initial conditions within the simulation domain at an estimated time in which the interim surface barrier was to be placed (July 1, 2007) were established using a two-step simulation. First, the uniform recharge rate was 3.5 mm/yr (Khaleel et al. 2004) before 1945, the year the tanks were deployed. Then, the simulation ran from 1945 to July 1, 2007, the time the interim surface barrier was to be installed, under the recharge rate of 100 mm/yr (Khaleel et al. 2004). Normally, such hydraulic conditions would be the same as at similar depths across the domain, but, because of the shedding effect caused by the impermeable tanks, water flowing around the tanks (i.e., represented by inactive nodes) created slightly different initial conditions in the vicinity of the tanks.

At time zero (i.e., July 1, 2007), the interim barrier was placed on the surface above Tanks T-105, -106, -108, and -109 as shown in Figure 2.1. The surface barrier was rectangular-shaped, and its size was 76×66 m [from (x_1, y_1) = (36, 36) m to (x_2, y_2) = (112, 102) m] with the longer sides orienting to the east-west direction. The surface barrier was simulated by changing the boundary condition inside the surface barrier to zero flux and keeping the boundary condition at 100 mm/yr outside the surface barrier. A water table was applied to the bottom boundary to mimic the water table beneath the T tank farm.

The effects of the interim surface barrier on soil-water conditions were shown by comparing soil-water variables at two locations, one inside the surface barrier [(x, y) = (81, 67) m] and the other outside the surface barrier [(x, y) = (15, 67) m]. As will be shown below, these effects are stronger at a shallower depth and weaker at a deeper depth.

2.3 Simulation Results

The time series and/or the spatial distribution of the simulated results of soil-water content, saturation, pressure head, and water flux are reported below.

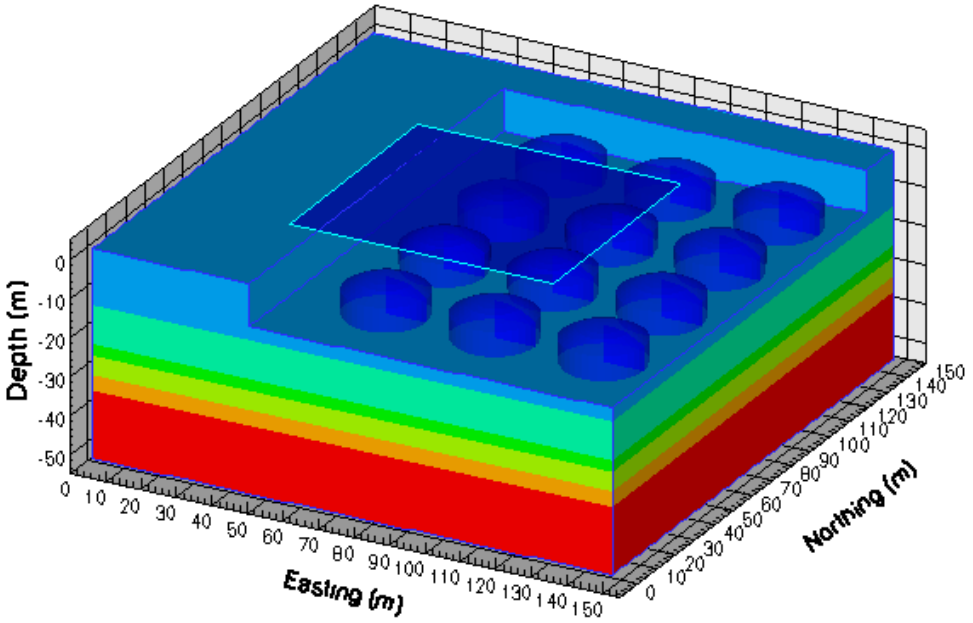

Figure 2.1. Simulation Domain Without and with an Interim Surface Barrier. The domain size was (x, y, z) = (148, 148, 55) m. The origin of the simulation domain in the Hanford coordinate system was (x_0, y_0) = (466710, 136650) m.

2.3.1 Time Series of Soil-Water Content

Figure 2.2 shows the time series of soil-water content inside [(x, y) = (81, 67) m] and outside [(x, y) = (15, 67) m] the surface barrier at four different depths. As expected, the soil-water content was stable through the simulation period outside the surface barrier. Inside the surface barrier, the soil-water content decreased with time. The water-content decrease ranged from 0.0 at the 25.5-m depth to 0.015 m^3m^{-3} at the 0.5-m depth 1 year after the placement of the surface barrier; 3 years after the placement of the surface barrier, the water-content decrease ranged from 0.005 m^3m^{-3} at the 25.5-m depth to 0.025 m^3m^{-3} at 15.5-m depth. Note that the slight difference in water content at the time the surface barrier was placed (Year 2007.5) was caused by the shedding effects of the impermeable tanks at depths of 15.5 and 25.5 m.

2.3.2 Time Series of Soil-Water Pressure Head

Figure 2.3 shows the time series of the soil pressure head inside [(x, y) = (81, 67) m] and outside [(x, y) = (15, 67) m] the interim surface barrier at four different depths. As expected, the soil-water pressure was stable through the simulation period outside the surface barrier. Inside the surface barrier, the soil-water pressure decreased (became more negative) with time. One year after the placement of the surface barrier, the soil-water pressure decrease ranged from 0.0 bar (0.0 m) at 25.5-m depth to -0.244 bar (-2.49 m) at 0.5-m depth; 3 years after the placement of the surface barrier, the soil-water pressure decrease ranged from -0.018 bar (-0.19 m) at 25.5-m depth to -0.407 bar (-4.15 m) at 0.5-m depth. Note that the slight difference in soil-water pressure at the time the surface barrier was placed (Year 2007.5) was caused by the shedding effects of the impermeable tanks at depths of 15.5 and 25.5 m.

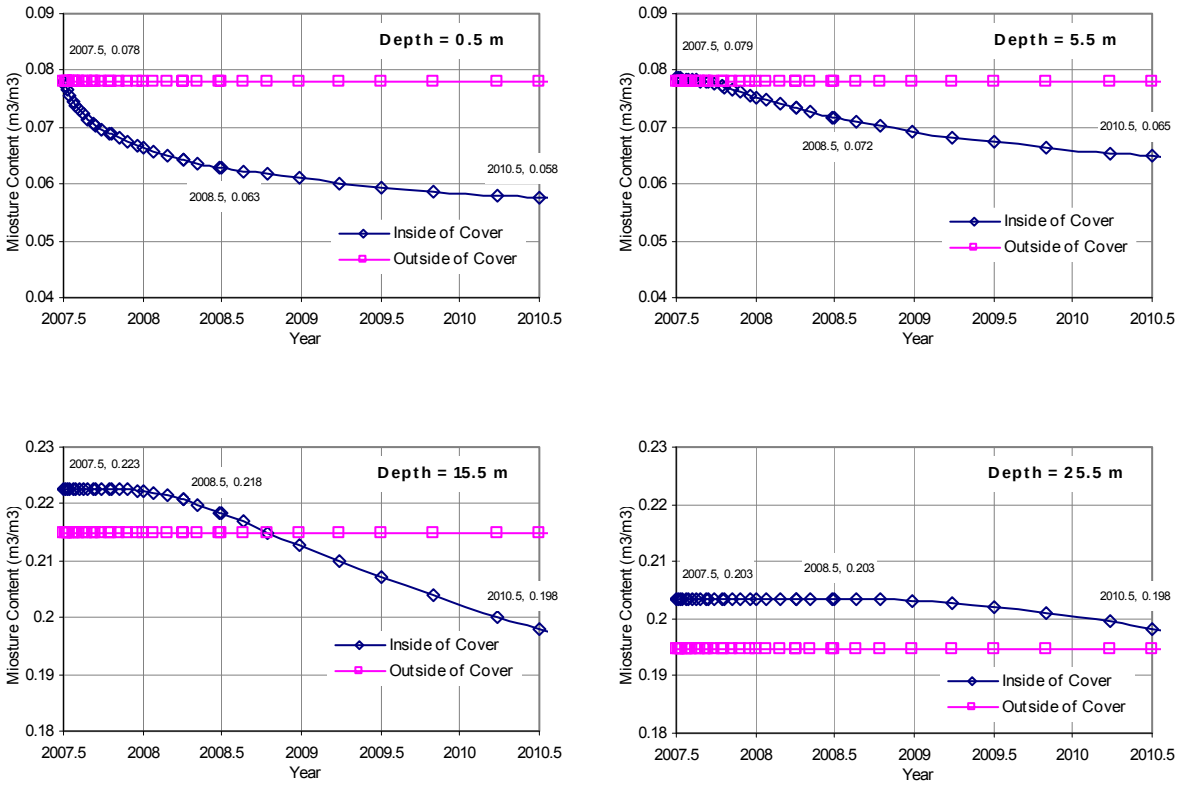

Figure 2.2. Time Series of Soil-Water Content Inside [(x, y) = (81, 67) m] and Outside [(x, y) = (15, 67) m] the Interim Surface Barrier at Four Different Depths. The numbers by the curves are times and soil-moisture contents at these times. The origin of the simulation domain in the Hanford coordinate system was (x0, y0) = (466710, 136650) m.

2.3.3 Time Series of Soil-Water Flux

Figure 2.4 shows the time series of the fluxes inside [(x, y) = (81, 67) m] and outside [(x, y) = (15, 67) m] the interim surface barrier at four different depths. As expected, the soil-water flux outside the surface barrier was stable through the simulation period. Inside the surface barrier, the soil-water flux decreased with time. One year after the placement of the surface barrier, the soil-water flux decrease ranged from 0.2 mm/yr at 25.5-m depth to 94.7 mm/yr at 0.5-m depth; 3 years after the placement of the surface barrier, the soil-water flux decrease ranged from 27.2 mm/yr at 25.5-m depth to 98.3 mm/yr at 0.5-m depth. Note that, at depths of 15.5 and 25.5 m, the slight difference in soil-water flux at the time the surface barrier was placed (Year 2007.5) was caused by the shedding effects of the impermeable tanks.

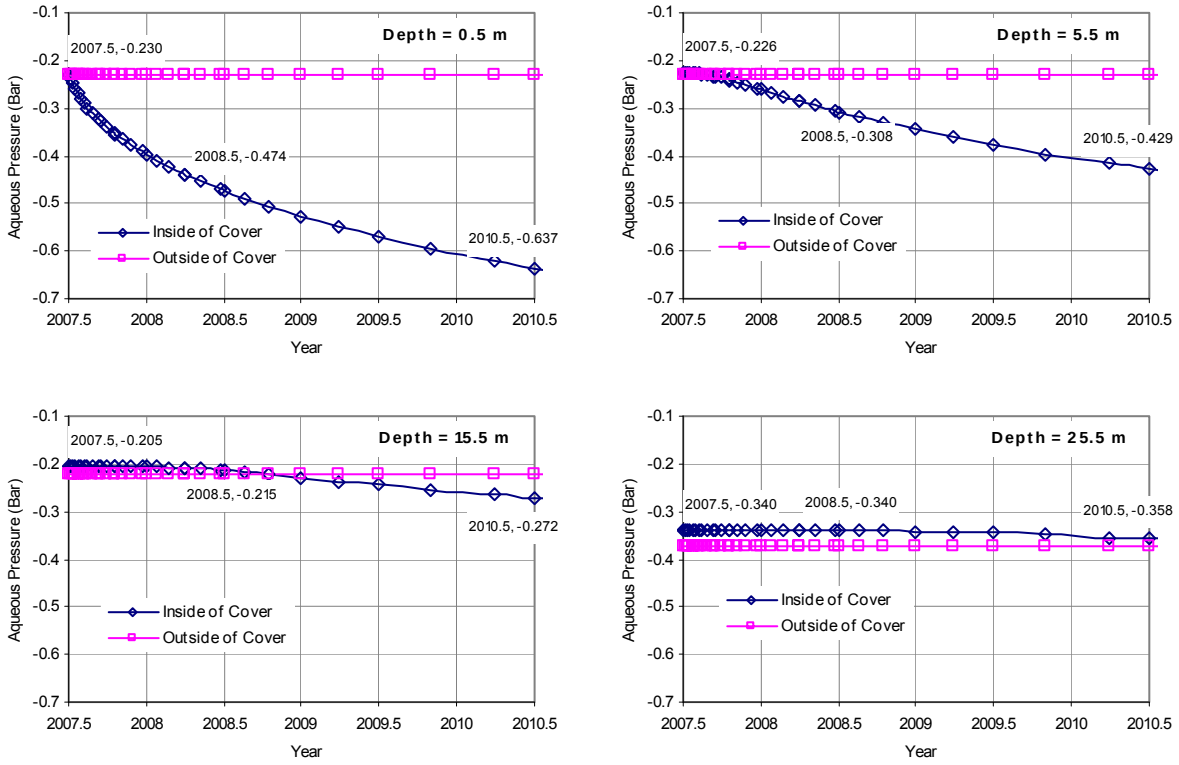

Figure 2.3. Soil-Water Pressure Inside [(x, y) = (81, 67) m] and Outside [(x, y) = (15, 67) m] the Interim Surface Barrier at Four Different Depths. The numbers by the curves are times and soil-water pressures at these times. 1 bar = 10.2 m H_2O height.

2.3.4 Spatial Distribution of Soil-Water Saturation

The spatial distributions of soil water are shown using two-dimensional contours of soil-water saturation in the selected horizontal planes and vertical planes at the time the surface barrier was applied (Year 2007.5) and 1, 2, and 3 years after the surface barrier was applied.

Figure 2.5 shows the horizontal distribution of soil-water saturation at a depth of 0.5 m in different times. At the time the surface barrier was placed (Year 2007.5), the soil water was uniform, except that it was slightly wetter at the places right above each of the tanks because of the tank shedding effect. After the surface barrier was emplaced, the soil beneath the surface barrier became drier gradually. Similar effects can be seen at the depth of 15.5 m (Figure 2.6).

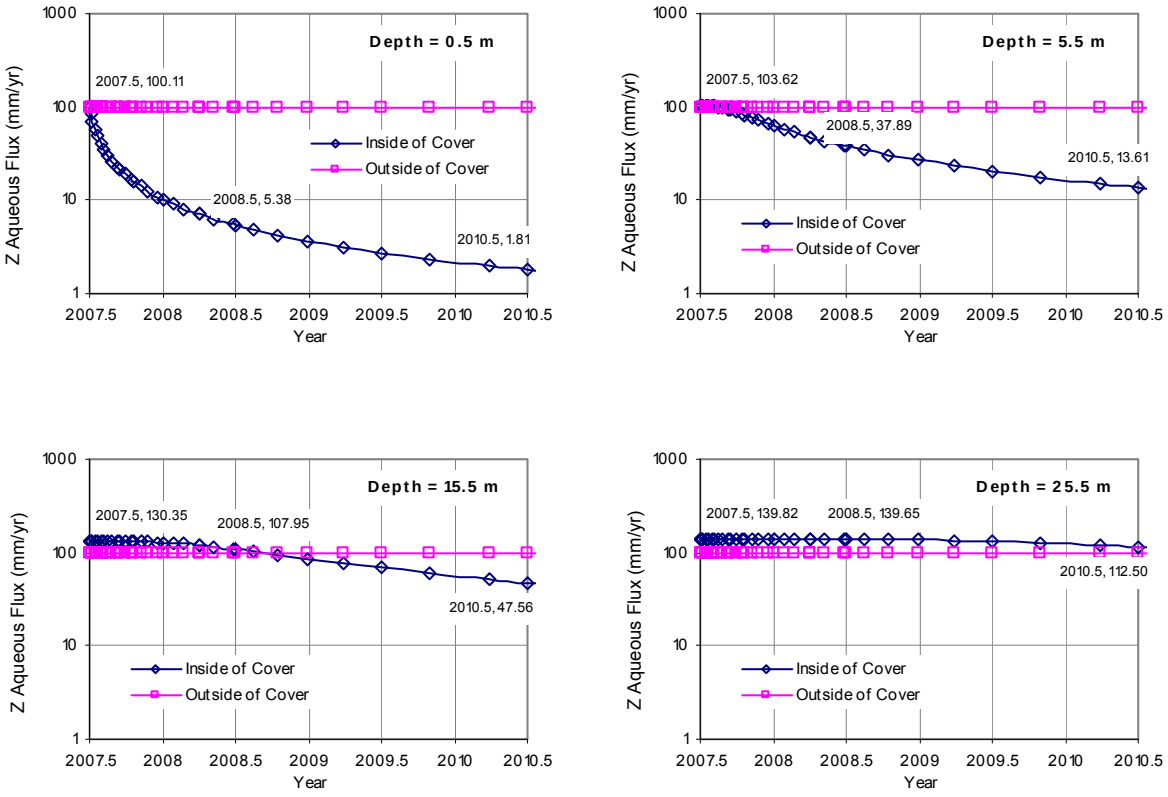

Figure 2.4. Soil-Water Flux Inside [(x, y) = (81, 67) m] and Outside [(x, y) = (15, 67) m] the Interim Surface Barrier at Four Different Depths. The numbers by the curves are times and soil-water fluxes at these times.

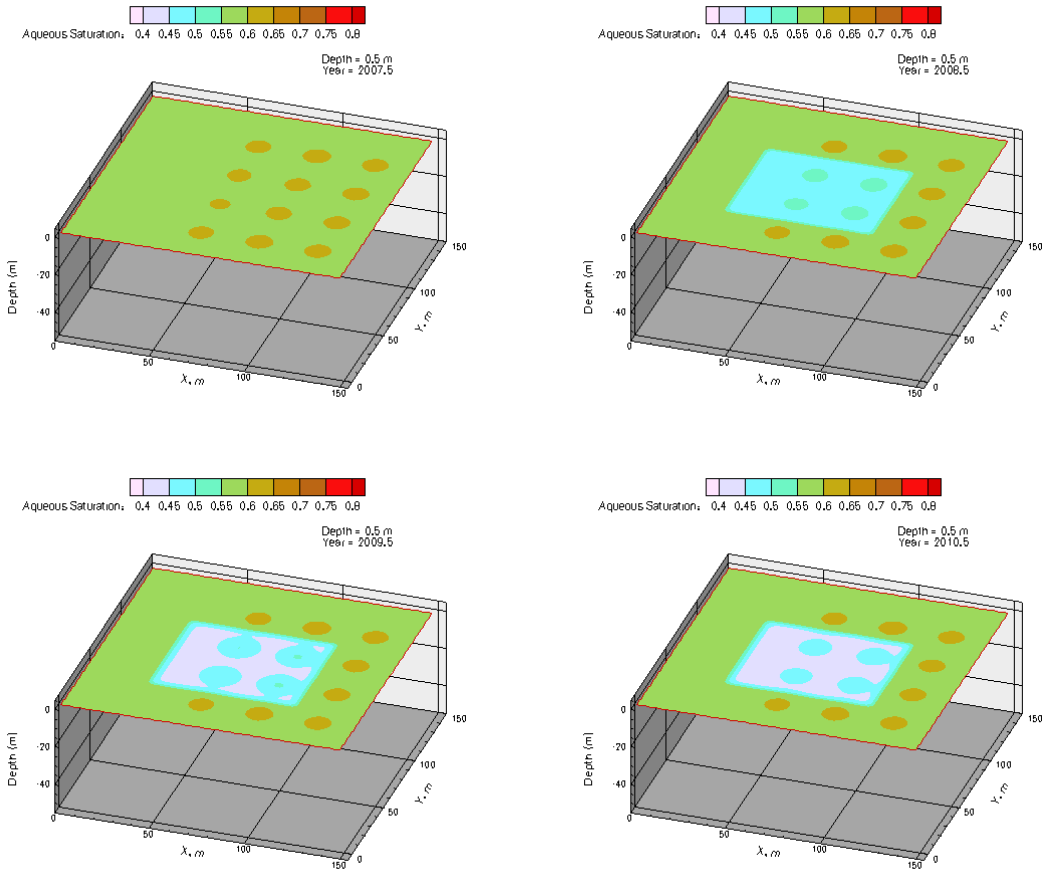

Figure 2.5. Horizontal Distribution of Soil-Water Saturation at Depth 0.5 m at Different Times. The interim surface barrier was emplaced in Year 2007.5.

Figure 2.7 shows the vertical distributions of soil-water saturation and stream lines at an easting transect crossing the center of Tanks T-104, T-105, and T-106. The soil beneath the surface barrier became drier gradually. The stream lines indicate that, as the soil beneath the surface barrier became drier, some water at the relatively wetter region beneath the place without a surface barrier moved laterally into the drier region beneath the covered region. This effect became stronger with time. This lateral movement of water is referred as the "edging effect." The results suggest that, 3 years after the placement of the surface barrier, the distance being affected beyond the edge of the surface barrier in the easting direction was about 5 m. Figure 2.8 shows vertical distributions of soil-water saturation and stream lines at an easting transect crossing the center between tank rows T-104, T-105, T-106 and tank rows T-107, T-108, and T-109. Similar results were observed in Figure 2.8 as those in Figure 2.7.

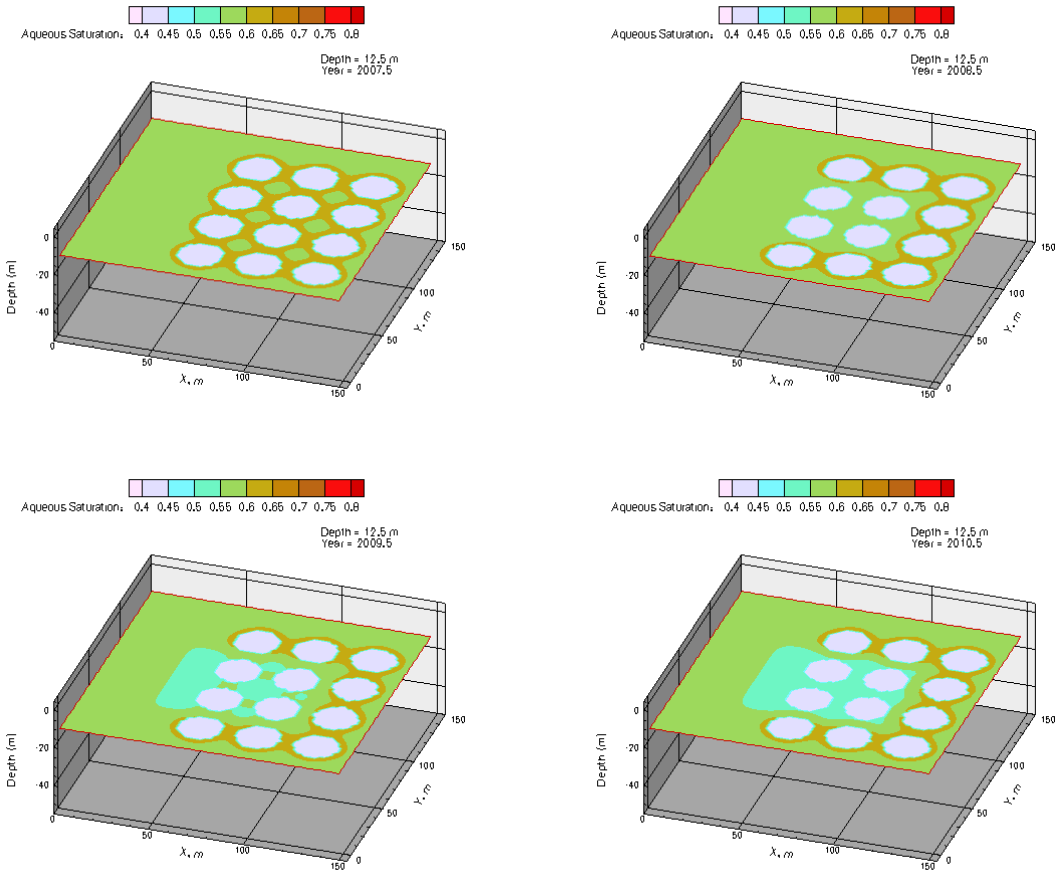

Figure 2.6. Horizontal Distribution of Soil-Water Saturation at Depth 12.5 m in Different Times. The interim surface barrier was emplaced in Year 2007.5.

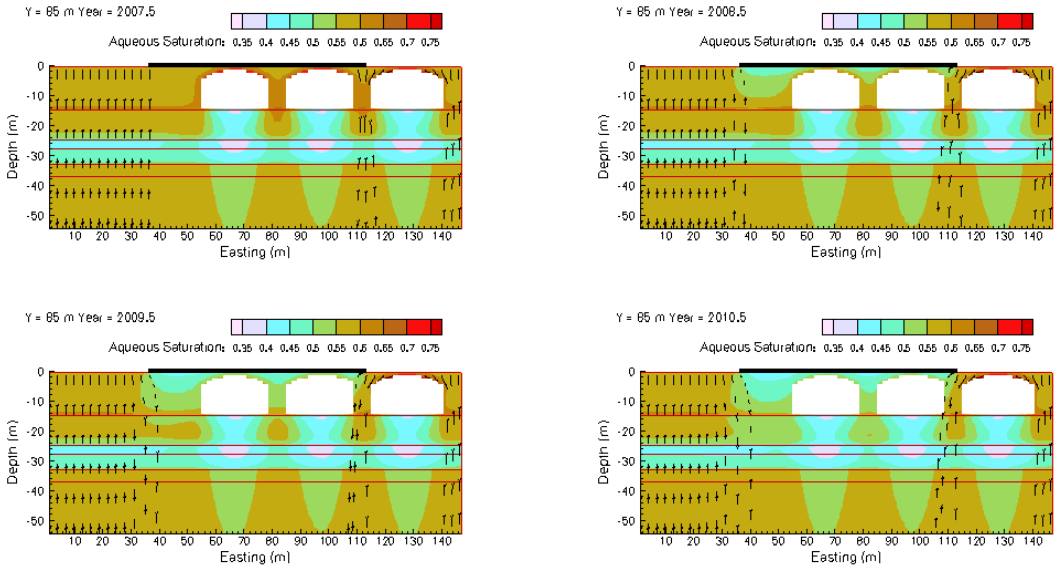

Figure 2.7. Vertical Distributions of Soil-Water Saturation and Stream Lines at an Easting Transect Crossing the Center of Tanks T-104, T-105, and T-106. The interim surface barrier was emplaced in Year 2007.5.

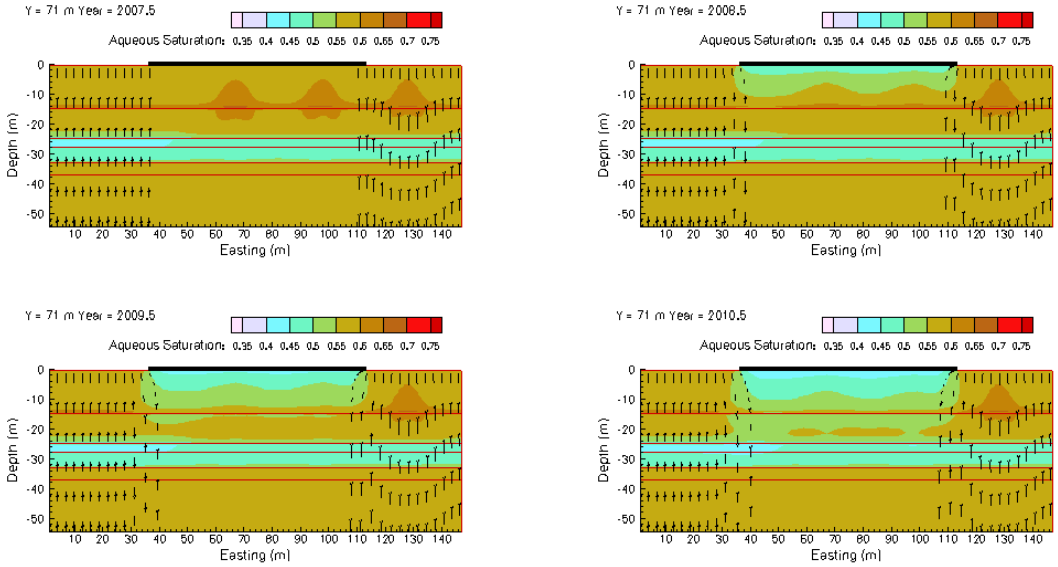

Figure 2.8. Vertical Distributions of Soil-Water Saturation and Stream Lines at an Easting Transect Crossing the Center Between Tank Rows T-104, T-105, T-106 and Tank Rows T-107, T-108, and T-109. The interim surface barrier was emplaced in Year 2007.5.

3.0 Monitoring Methods and Equipment

This section describes the criteria used to select the various measurement methods, the principals of selected methods, and the description of the selected instruments.

3.1 Soil Water and Environmental Variables

Variables to be monitored are chosen based on their contribution to describing soil-water flux conditions and inputs. Principal variables to be monitored are 1) soil-moisture content, 2) soil-water pressure, and 3) soil-water flux. Soil-water content shows the actual moisture contained in the soil. Soil-water content ranges between zero and the porosity of the soil. Soil-water pressure (or head) describes the energy level of soil water and is of primary importance in determining the state and movement of water in the soil. Differences in the soil-water head between one point and another give rise to the tendency of water to flow within the soil. Soil-water pressure in the vadose zone is often negative due to the suction of soil particles on water. Unless the soil is very dry, the pressure head generally varies logarithmically from zero when the soil is fully saturated to a few bars (negative pressure) when soil drainage has effectively ended. Both soil-water content and pressure describe the static state of soil water. Soil-water flux describes the dynamic state of soil water, showing how fast soil water moves in the soil. The reasons for monitoring all three types of variables are summarized below.

- Each variable reflects one aspect of the soil-moisture regime.
- Their variation is different under different conditions. On the one hand, the change of water content can be measured more easily than the change of pressure head under relatively wet conditions. On the other hand, the change of pressure head can be measured more easily than the change of water content under relatively dry conditions.
- Soil-water flux is directly related to the transport velocity of the dissolving solute. However, due to very small values, especially in arid regions (e.g., on the order of a few to a few tens of mm/yr at Hanford), the measurement is often difficult. With the emergence of a new measuring technique, water flux as low as 1 mm/yr is measurable in coarse textured soils.

Secondary variables to be monitored include soil temperature and meteorological conditions, including precipitation and air temperature. The measured precipitation will be used to estimate the total volume of water intercepted by the surface barrier.

3.2 Criteria for Method Selection

Table 3.1 illustrates criteria for selecting monitoring methods that were modified from criteria described by Everett et al. (1984). The criteria provide for a systematic way of determining which monitoring technologies will best serve the given objectives. Because of restrictions of working within the T tank farm, considerable attention was given to potential installation problems and constraints when selecting methods. For example, the segmented time-domain reflectometry probe was considered to measure water content. Due to the significant impacts of temperature on probe response and to impacts of cable length on signal strength, this probe was eliminated. The cone-penetrometer was also considered to measure soil-water pressure head, but this method was also eliminated because of its possible insufficient strength in gravelly soil. While the selected technologies may not meet all criteria, they do encompass the majority of criteria presented.

Table 3.1. Criteria For Selecting Alternative Vadose Zone Monitoring Methods

Item	Criteria	Neutron Probe	Capacitance Probe	HDU	Drainage Gauge
1	Applicability to Tank Farm	Yes	Yes	Yes	Yes
2	Measurement accuracy	±0.016 cm^3cm^{-3}[a]	±0.01 cm^3cm^{-3}[b]	±20%[c] ±0.25ºC[d]	±10% [1 ml resolution][e]
3	Measurement range	Zero to full saturation	Zero to full saturation	-0.1 bar (-1 m) to -10 bar (-100 m)[f]	1 to 1000 mm/yr
4	Representative volume	~0.04 to ~0.7[g] m^3	~ 0.002[h] m^3	1.1E-5[i] m^3	~1.7[j] m^3
5	Limitations	Cannot be automated	Difficult to install for large depth	Difficulty to replace once in place	Soil must be disturbed; not applicable to very dry soil[k]
6	Cost	High	Medium	Low	Medium
7	Potential installation problem	Bending access tube	Inappropriate refilling of annulus	Bad soil-sensor contact	Inappropriate density of backfill
8	Data collection system/ wire length effects	Manual/ No	Automated/ No	Automated/ Negligible	Automated/ No
9	Continuous or discrete sampling	Discrete	Continuous	Continuous	Continuous
10	Maintenance requirements	Minor	Minor	Minor	Minor
11	Effect of hazardous waste on measurement	No	No	No	No
12	Power requirements	Battery	Battery	Battery	Battery
13	Multiple use capabilities	No	No	Yes	No
14	Other concerns	Radiological Exposure	No	No	No

(a) D. Carter, CPN International, Inc., personal communication, May 24, 2006.
(b) Campbell Scientific, Inc. (CSI 2006b).
(c) Calibration dependent. Accuracy value taken from Reece et al. (1996).
(d) J. Ritter, CSI, personal communication, June 2, 2006.
(e) D. Cobos, Decagon, personal communication, May 24, 2006.
(f) Reece et al. (1996).
(g) Calculated based on the information from the International Atomic Energy Agency (IAEA) (1970).
(h) Calculated based on the information from the user's manual (CSI 2006a).
(i) This is the volume of the HDU.
(j) This is the volume of the drain gauge.
(k) Water suction of the soil near the wick inside the fluxmeter must be smaller than the length of the wick.

Based on the criteria in Table 3.1, equipment such as a neutron probe, capacitance sensors, HDUs, and water flux meters are being used to monitor flow regime. A rain gauge is also installed to more accurately record precipitation, especially for storms. All the equipment except the neutron probe will be connected to data loggers, which remotely transmit data to a computer. The following sections describe the principle of each method and specific equipment chosen.

3.3 Water Content

Moisture content as a function of depth will be measured to monitor the impacts of the interim surface barrier in reducing water flux from baseline conditions. Soil-water measurements will be used to track wetting and drying processes and produce estimates of water fluxes using available soil-water potential data and soil hydraulic properties. Two methods, neutron moisture probe and capacitance probe, will be employed to monitor absolute or relative soil-moisture content. This affords the benefit of providing certain data through redundancy while at the same time offering advantages presented by each method. Additionally, both methods of measurement provide the accuracy (Table 3.1) needed to capture the predicted changes in soil-moisture content after the interim surface barrier is in place.

3.3.1 Neutron Probe Method

3.3.1.1 Principles

Neutron thermalization, as a method to measure soil-water content, uses a radioactive source of fast neutrons (mean energy of 5 MeV) and a detector of slow neutrons (~0.025 eV). High-energy neutrons emitted from the source are either slowed through repeated collisions with the nuclei of atoms in the soil (scattering) or are absorbed by those nuclei. The most common atoms in soil (Al, Si, and O) scatter neutrons with little energy loss. If the neutron hits an H atom, its energy is reduced on average to about half because the mass of the H nucleus is the same as that of the neutron. The concentration of thermal neutrons changes mainly with the H content of the surrounding material, while changes in H content occur mainly because of changes in soil-water content. Therefore, the concentration of thermal neutrons surrounding a neutron source placed in the soil can be precisely related to the soil volumetric water content.

A profiling type neutron moisture meter has a readout and control unit connected by cable to a cylindrical probe that is lowered into a borehole that is usually cased with an access tube. The probe is lowered into the tube and stopped at intervals to measure the thermal neutron concentration at that depth. The measurement volume is approximately a sphere with a radius of about 0.15 m in a wet clay soil and up to 0.5 m if the water content declines to 0.02 m^3m^{-3} (van Bavel et al. 1956).

3.3.1.2 Neutron Probe

Any type of neutron probe that has been calibrated can be used to measure soil-water content. An example is the 503DR hydroprobe (Figure 3.1) manufactured by CPN International, Inc. (Martinez, CA). The 503DR hydroprobe has a history of successful use at Hanford and is currently used for a number of Hanford waste site soil-moisture monitoring programs (DOE 2005; Ward et al. 2000). The probe includes a 50-mCi americium-241 and beryllium source and a neutron detector. The 16-sec neutron counts are recorded at different depths of 1-ft intervals. Operation of the Hydroprobe should follow the "Tank Farm Plant Operating Procedure—Operate Model 503DR Hydroprobe Neutron Moisture Detection" (Ross 2007).

3.3.2 Capacitance Method

Figure 3.1. 503 DR Hydroprobe

Capacitance, as an electromagnetic method to measure soil-water content, was introduced in the 1930s (Smith-Rose 1933) and developed rapidly with recent advances of microelectroncs in the 1990s (Paltineau and Starr 1997). According to Starr and Paltineanu (2002), positive features of capacitance probes include robust and stable instrumentation, fast response times, accuracy with good soil-probe contact, ease of use, safety, availability of several sensor configurations, and amenability to automatic and continuous logging over large areas (up to 500-m radium).

3.3.2.1 Principles

To measure the volumetric soil-water content (θ_v), the capacitance method uses the soil surrounding the electrodes as part of a capacitor in which the dipoles of water in the soil become polarized in response to the frequency of an imposed electric field. Capacitance probes consist of a capacitor connected to circuitry that oscillates at a frequency (F) that is dependent on the inductance (L) of an inductor and the total capacitance (C) of the electrode-soil system. For a given probe, the value of L is constant, and the value of C is related to the bulk dielectric constant (ε_{ra}) of the surrounding soil:

$$C = g\varepsilon_{ra} \tag{3.1}$$

where g is a geometrical constant based on the electrode configuration (size, shape, and distance between electrodes). The output of the capacitance probe is the oscillation frequency, which is an inverse square root function of the total capacitance:

$$F = \left(2\pi\sqrt{LC}\right)^{-1} = \left(2\pi\sqrt{gL\varepsilon_{ra}}\right)^{-1} \tag{3.2}$$

The total capacitance of the soil is a function of volumetric soil-water content (θ_v). Hence, oscillation frequency is a function of soil-water content.

The probe geometric constant, g, is often instrument-dependent. For one calibration equation to cover all the sensors and to allow one sensor or probe to be replaced at the same field position without loss of data continuity, a normalization process is used to minimize instrumental-dependent readings. For cylindrical sensors, a scaled frequency (S_f) is calculated by incorporating the raw-frequency reading in soil (F) with frequency readings in air (F_a) and in water (F_w) (Paltineanu and Starr 1997):

$$S_f = \frac{F_a - F}{F_a - F_w} \tag{3.3}$$

The relationship between S_f and soil-water content can be determined empirically. Sentek Pty Ltd (2001) calibrated the capacitance using a power function:

$$\theta_v = \left(\frac{S_f - c}{a} \right)^{\frac{1}{b}} \tag{3.4}$$

where a, b, and c are constants.

The zone of influence has both axial (vertically along the sensor) and radial (perpendicular to the sensor) components. The extent and shape of the primary zone of influence is largely dependent on the sensor geometry. Paltineanu and Starr (1997) found the axial zone of influence to be ±5 cm, centered at the plastic ring between the two metal rings, and the radial zone of influence to be primarily within 10 cm of the access pipe. Both axial and radial sensitivities were affected by soil-water content and scaled frequency. This suggests the importance of good probe installation.

Figure 3.2. (a) EnviroSMART Probe; (b) Field Installation

3.3.2.2 EnviroSMART Soil-Water Content Profile Probes

The capacitance probe to be used is a profile-type probe distributed by Campbell Scientific, Inc. (CSI, Logan, UT). It is called an EnviroSMART probe (CSI 2006a, b) and is made by Sentek Pty Ltd (Stepney, Australia). It consists of a probe with several independent sensors and an access tube (Figure 3.2).

EnviroSMART Probe:

- Multiple sensors with flexible depth placement (10-cm increments)
- Can monitor from shallow depths (0 to 10 cm) to deep installations (up to 30 meters)
- Length of EnviroSMART probe can be customized to suit a wide range of applications
- Up to 16 sensors per probe
- In-built probe orientation and depth settings to increase sensor repeatability

- A range of connectivity for integration is available, including SDI-12, voltage output, current output, RS-485 (Modbus), and RS-232 (Modbus).

Access Tube:

- Customized access tube increases sensor accuracy
- Sensors have no direct contact with the soil
- Specially sealed to guarantee long-term operation
- No preferential path flow of water alongside the probe body
- Probe and sensors are readily accessible and serviceable without destroying the site
- Easily change sensor configuration
- Minimized soil and root disturbance
- Data continuity.

3.4 Soil Matric Potential and Heat Dissipation Unit Method

Soil-water-pressure measurements can be used to track wetting or drying processes, identify pressure gradients, and produce estimates of water fluxes using available soil-water-content data and soil hydraulic properties.

An HDU can be used to indirectly measure the soil matric potential (ψ_s) by measuring the thermal conductivity (k) of the reference matrix, which is part of an HDU and often is made of porous ceramics. The water content of the ceramic matrix (θ_{vc}) changes with the matric potential of the ceramic matrix (ψ_c) and causes a corresponding change in k. Because the equilibrium between the sensor and the soil is a matric potential (i.e., $\psi_s = \psi_c$) rather than a water-content equilibrium, the measured thermal conductivity of the reference matrix is related to the matric potential of the soil. HDU measurement and calibration are independent of soil texture because the heat pulse is restricted to the ceramic. It is also independent of salinity because the method is independent of electrical conductivity.

3.4.1 Principles

HDUs consist of a heater and a temperature sensor in a porous matrix material. The HDU is heated for a fixed time period. The rate of heat dissipation is controlled by the water content of the porous matrix because water conducts heat much more readily than air. The temperature increase measured by the temperature sensor at time t represents the heat that is not dissipated at this time. The time dependence of temperature, T, in a line heat source buried in an infinite medium can be approximated by Shiozawa and Campbell (1990):

$$T - T_0 = \frac{q}{4\pi k} \ln(t - t_0) \tag{3.5}$$

where T_0 is the initial temperature, q is the heat input, and t_0 is an offset time. Heat dissipation is generally determined as the difference between two temperatures, one measured after 1 s of heating and the other measured after a heating time that can vary from 20 to 30 s (CSI HDUs). Whatever time period is chosen for laboratory calibration should also be used for field monitoring.

Due to the variability of the heat-transfer properties of individual HDUs, the relationship between temperature increase and matric potential is sensor-dependent. Flint et al. (2002) evaluated calibration equations for six HDUs and suggested normalizing the temperature increase according to:

$$S_{\Delta T} = \frac{\Delta T_d - \Delta T}{\Delta T_d - \Delta T_w} \tag{3.6}$$

where $S_{\Delta T}$ is the scaled temperature rise, ΔT is the temperature increase, and subscripts "d" and "w" denote the temperature increases for a dry and water-saturated ceramic matrix, respectively. This relation results in a range of 0 to 1 for dimensionless temperature. The matric potential is related to the dimensionless temperature rise by an empirical model.

The heat conductivity of the HDUs is temperature dependent, and thus, the measurements that deviate from a reference temperature need to be corrected to the reference temperature. Flint et al. (2002) developed the following equations to correct for temperature effects for HDUs calibrated at 20°C:

$$S^*_{\Delta T} = S_{\Delta T} - s(T - 20) \tag{3.7a}$$

$$s = c_0 + c_1 S_{\Delta T} + c_2 S^2_{\Delta T} + c_3 S^3_{\Delta T} + c_4 S^4_{\Delta T} + c_5 S^5_{\Delta T} \tag{3.7b}$$

where $S_{\Delta T}^*$ = corrected $S_{\Delta T}$
s = an intermediate variable
T = the field temperature
c_0 = 0.0013
c_1 = 0.011
c_2 = 0.0203
c_3 = -0.0747
c_4 = 0.0559
c_5 = -0.0133.

The upper measurement range of the HDUs is controlled by the air-entry pressure (bubbling pressure) of the matrix material of the probe, which is generally -10 kPa (-1 m). Matric potentials above the air-entry pressure (i.e., between 0 and -10 kPa [-1 m]) cannot be measured because the matrix material is essentially saturated. The lower measurement limit is generally considered to be about -1 MPa (-100 m) (Reece 1996). However, less-accurate measurements can be made between -1 and -35 MPa (-100 and -3500 m).

It is critical to maintain good hydraulic contact between sensors and surrounding soil in the field. Good contact may be difficult to attain in very coarse sediments, such as gravel. Wet silica flour is often used during installation to confirm that there is good contact between the sensor and surrounding soil. Fredlund et al. (2000) found that HDUs do not provide reliable matric-potential measurements in freezing or thawing soils because the voltage drops as a result of the effect of the latent heat of fusion on thermal conductivity. However, freeze-thaw cycles did not affect the capability of HDUs to function upon return to normal conditions.

The heat-dissipation method as currently applied requires constant power dissipation at the heating element. A constant voltage source cannot be used in place of a constant current source because there is a voltage drop in the cable. Thus, if a voltage source were used, different calibrations for sensors with different cable lengths would be required. Variation in applied power during measurement or between measurements will cause the temperature increase to change, thus introducing an error in application.

3.4.2 CSI 229 HDU

The HDU to be used is made by Campbell Scientific, Inc. and is called the "229 Heat Dissipation Matric Water Potential Sensor" (Figure 3.3). The sensor has a cylindrically-shaped porous ceramic body. A heating element that has the same length as the ceramic body is positioned at the center of the cylinder. A thermocouple is located at mid-length of the ceramic and heating element. The position of the heating element and the thermocouple is maintained by placing both inside a hypodermic needle, which also protects the delicate wires. The volume inside the needle, which is not occupied by wiring, is filled with epoxy.

HDUs provide affordable measurements of soil matric potential and also the added benefit of measuring soil temperature. The size of a single HDU is also a benefit, with the CSI HDU (Model 299) dimensions being 1.5 cm in diameter and 60 mm in length.

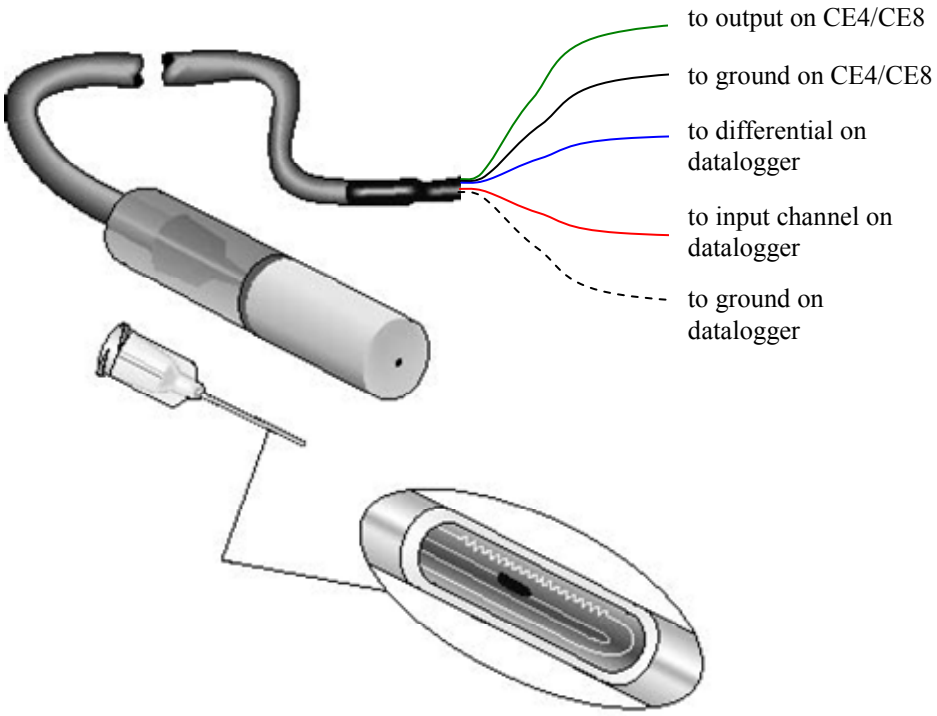

Figure 3.3. A 229 Heat-Dissipation Matric Water Potential Sensor is shown at the top (the dashed line is in clear color). The hypodermic assembly (without epoxy and ceramic) is shown just below. A cutaway view shows the longitudinal section of the needle with heater and thermocouple junction.

Using the 229 sensor requires a power source that is a constant current source. This can be achieved by using CSI's CE4 or CE8 current excitation modules, which provide regulated outputs of 50±0.25 mA. The –L option on the model 229 sensor indicates that the cable length is user specified. The 229 sensor is compatible with the 21X, CR7, CR10(X), CR23X, CR800, CR1000, and CR3000 dataloggers.

3.5 Water Flux Meter

A soil-water balance takes into consideration the inputs, losses, and storage of water in a soil profile. An important component of the water balance is the water that drains from the bottom of the soil profile, referred to as drainage. This is water that has gone sufficiently deep that it cannot be removed from the soil by transpiration or evaporation. This drainage moves downward with dissolved contaminants. If there is no drainage, then there would be no convective movement of contaminants. The other components of the water balance can be measured, but the deep drainage typically has been computed as the remainder when the other components were measured and accounted for. Because of uncertainties in the measurements of the other water-balance components, the calculated drainage is subject to large errors.

3.5.1 Principles

Gee et al. (2002) designed, constructed, and tested a water fluxmeter to directly measure drainage fluxes in field soils. The fluxmeter, which was designed to minimize divergence, concentrates flow into a narrow sensing region filled with a fiberglass wick. The wick applies suction, proportional to its length, and passively drains the meter. The meter can be installed in an augured borehole at almost any depth below the root zone. Water flux through the meter is measured either with a self-calibrating tipping bucket, or with a dosing siphon whose action is monitored with a small capacitance probe (see Figure 3.4). Under proper conditions, water fluxmeters have the capability of providing continuous and reliable monitoring of unsaturated water fluxes ranging from less than 1 mm yr^{1} to more than 1000 mm yr^{-1}.

3.5.2 Decagon Drain Gauge

The drain gauge is installed below the root zone. Water infiltrates down through the divergence control tube and then is pulled by gravity down a fiberglass wick into a collector. As collected water fills the measurement reservoir, the water level is monitored by a water-depth sensor. When the water level in the measurement reservoir reaches the top of the siphon tube, the water empties, and the event is recorded by an attached data logger. The emptied water then drains into the sampling reservoir. A sampling syringe, attached to the water reservoir sampling port (blue tube), can draw water samples out of the sampling reservoir for chemical analysis. Excess water drains out of an overflow port and into the soil while allowing a volume of water to remain for sampling.

The drain gauge's water-level sensor comes with a 3.5-mm "stereo-plug" style connector. This allows for rapid connection directly to a data logger.

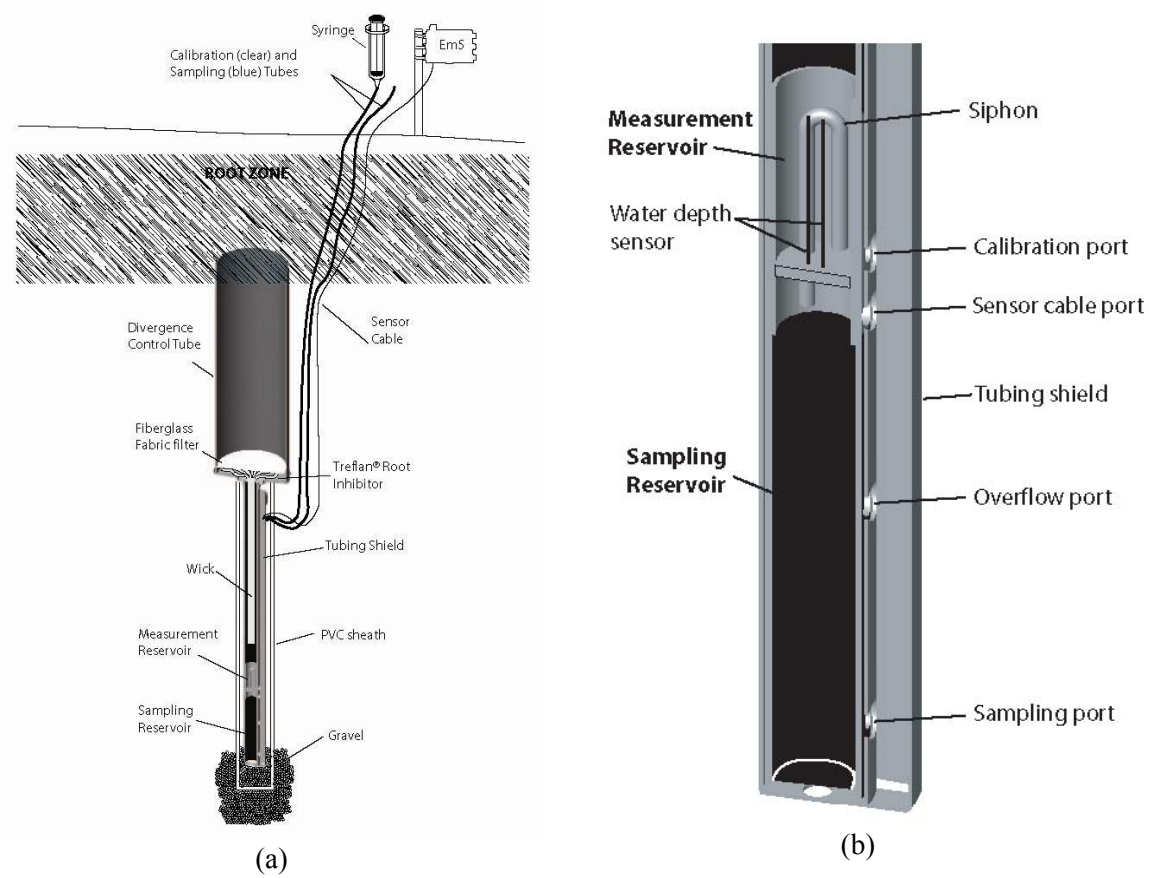

(a) (b)

Figure 3.4. (a) Decagon Drain Gauge; (b) Close-up of Measurement Section (Decagon Devices, Inc. 2006)

3.6 Precipitation and Air and Soil Temperatures

Precipitation and air temperature will be continuously monitored using a single meteorological station. Monitoring precipitation directly at T tank farm is useful in determining the total amount of meteoric water and the amount of water intercepted by the surface barrier. Localized thunderstorms that occasionally occur at Hanford produce spatially variable short-term, high-energy precipitation events. Such events require that a meteorological monitoring station be located at the T farm to document potential localized precipitation events. Site-specific measurement of precipitation will be used to assess the quantity of precipitation intercepted by the barrier.

Power requirements necessary for a heated rain gauge necessitated that the rain gauge not be heated because there is no AC power in the Tank Farm. As such, the rain gauge may not accurately measure precipitation during periods of snowfall. Given the proximity of the Hanford Meteorological Station (HMS) and the uniformity of snowfall across the Hanford Site, it is acceptable to conclude that snowfall measured by the HMS will approximate describe the snowfall at the T farm. Table 3.2 gives the manufacturer's documented instrument accuracy along with summarizing the rationale for using the chosen monitoring method.

The soil temperature will be measured and recorded during set time intervals at various locations. Measuring soil temperature provides information on soil-temperature gradients that contribute to liquid water and vapor movement in the subsurface. Automated soil-temperature measurements will be made using HDUs, which provide measurements of both soil temperature and soil-water pressure. HDUs provide for an efficient method to measure soil temperature, given that they will already be used for measuring soil-water pressure.

Table 3.2. Selected Methods to Monitor Meteorological Conditions and Selection Rationale

Selected Monitoring Method(s)	Manufacturer	Accuracy	Rationale
Rain gauge	Texas Electronics (distributed by CSI)	±1%[(a)]	Standard methods. Capable of continuous automated measurements.
Thermometer	CSI	±0.1°C[(b)]	
(a) (CSI 2002). (b) (CSI 2006c).			

3.7 Electric and Electronic Equipment

The measurement and control device for the HDUs, capacitance probes, drain gauge, and meteorological station will be the CR10X or other compatible datalogger manufactured by CSI (Logan, UT). The datalogger allows the data to be measured, processed, stored, and retrieved. However, permanent power does not exist near the proposed placement of the data logger. This requires that the data logger and peripherals be powered by a battery that can be recharged with a solar panel.

For automatic monitoring and data collection, compatible electric and electronic equipment are needed. Table 3.3 summarizes this equipment and its functions.

Table 3.3. Electric and Electronic Equipment and their Function

Equipment/Instrument	Functions
Datalogger	Data collection and storage
Rechargeable Battery w/charger	Power supply
Solar Panel w/cable	Power source for the rechargeable battery
Mulitiplexer	To connect to multiple HDUs
Excitation Module	Create a constant current power source for HDU
Network Link, Radio, Antenna, interface	Wireless data communication
Software	Software to control the datalogger

4.0 Equipment Calibrations

All monitoring equipment to be installed at T Tank Farm will be verified to be functioning before field installation. For the temperature sensors, rain gauge, and drain gauges, sensors arrived calibrated to relate sensor output to the measurement parameter. The neutron probe, capacitance probes, and HDUs do not come from the manufacturer with the necessary calibration or normalization information, requiring that instrument normalization be performed (capacitance probes and HDUs) and calibrations be developed (neutron probe and HDUs). This section documents the instrument verifications and calibrations in addition to sensor normalizations.

4.1 Neutron Probe

The neutron probe to be used in the monitoring will measure relative soil wetness, which is proportional to but not equal to the absolute soil-water content. Additional neutron calibration model may be developed to enhance the quantification of soil water content. The relative soil wetness between different locations will still be comparable to show the impact of the surface barrier on soil-water regime.

4.2 EnviroSMART Capacitance Probe

Two components exist as part of the EnviroSMART capacitance probe calibration. First is normalization or scaling of the EnviroSMART capacitance sensor output. Due to slight sensor-to-sensor variations, normalization is necessary to allow for direct comparison of results from each capacitance sensor and also allows for a single calibration to be used to relate sensor output to volumetric moisture content. The second component is the actual calibration, which is developed using scaled sensor response and associated moisture content.

Normalization: Normalization is performed by measuring the response of each sensor in open air and when surrounded by water. The normalization procedure is thoroughly documented in Appendix B of the EnviroSMART user's manual (CSI 2006a). For that reason, details of the method are not duplicated here. The values obtained from the open-air and water measurements are used to normalize sensor output using Eq. (3.3).

The open-air measurements were performed while holding the probe out at arm's length into the air, verifying that the sensors are a distance away from any other objects that may affect the measurement. The water measurements were taken with the sensors inside the water-tight access tube that was placed in a 10-in.-diameter cylindrical water vessel (Figure 4.1). Table 4.1 presents the water and open-air measurement output for each sensor.

Figure 4.1. Water Vessel and Access Tube for Capacitance Sensor Normalization Measurement in Water

Table 4.1. Capacitance Sensor Frequency Response in Air and Water. Values are used to normalize capacitance sensor output using Eq. 2.3.

Sensor Serial #	Frequency		Sensor Serial #	Frequency	
	Air	Water		Air	Water
AP06-303	37584	28503	FE06-374	37720	28468
AP06-304	37170	28219	FE06-375	37180	27835
AP06-305	37522	28657	FE06-376	37162	28246
AP06-309	37728	28863	FE06-377	37468	28374
AP06-310	37583	28413	FE06-378	37545	28517
FE06-371	37448	28395	FE06-379	37359	28270
FE06-372	37048	28148	FE06-380	37381	28456
FE06-373	37323	28227			

Calibration: The capacitance probe calibration documentation (Sentek Pty Ltd. 2001) provides a default calibration developed using sand, loam, and clay-loam soils. This calibration was developed by performing nonlinear regression on frequency data for paired volumetric moisture content and capacitance sensor scales (Figure 4.2). The default calibration is sufficient to show relative changes in soil-water content, which is the primary interest in this study. The manufacturer's developed calibration follows the form,

$$\theta_v = \left(\frac{S_f - c}{a} \right)^{\frac{1}{b}} \tag{4.1}$$

where a is 0.1957, b is 0.404, and c is 0.02852.

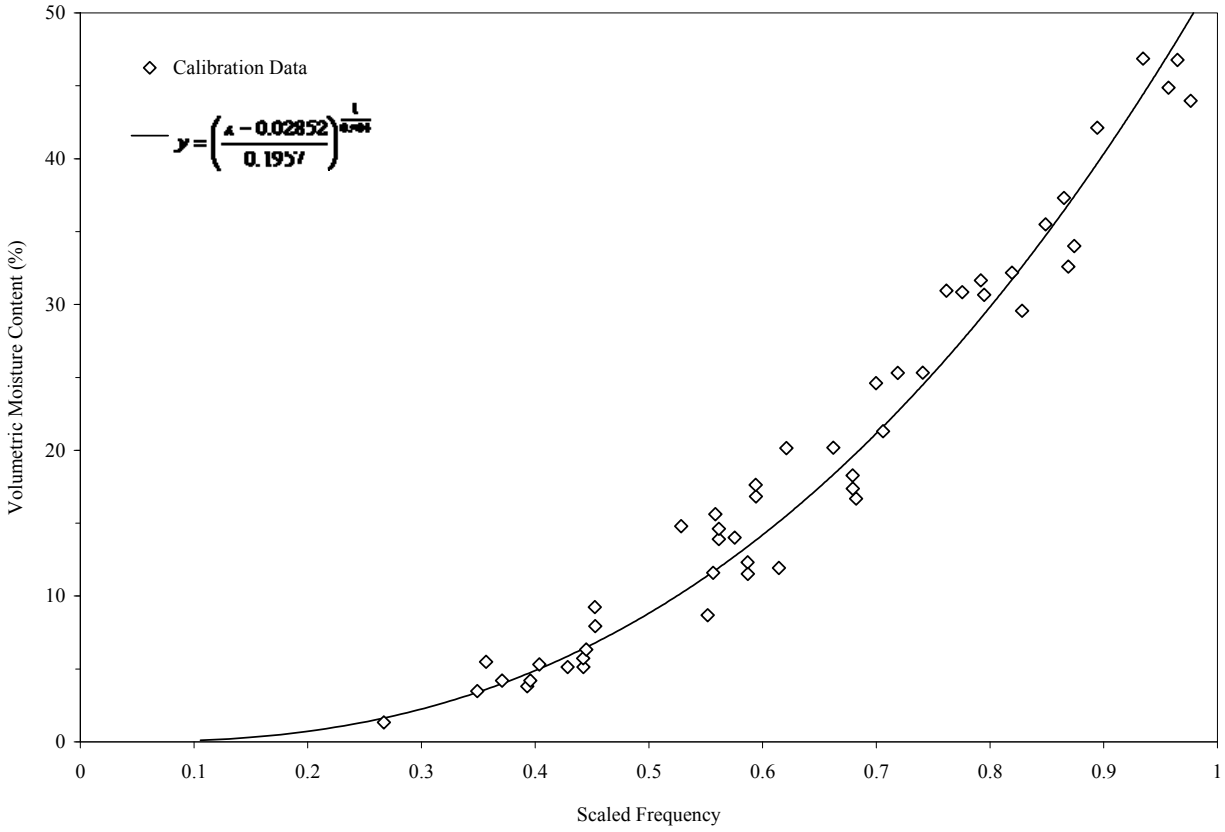

Figure 4.2. Capacitance Probe Default Calibration (Sentek Pty Ltd 2001)

4.3 Heat-Dissipation Unit

As explained by Scanlon et al. (2002), a variety of procedures can be used to calibrate heat-dissipation sensors. The sole requirement is that the matric potential of the medium surrounding the sensor be known. Similar to the capacitance probe, there are two elements to the HDU calibration: 1) a normalization procedure to remove variation between the HDU sensors (the normalization of temperature rise is sensor specific, and thus all sensors need to be normalized) and 2) a calibration procedure to develop the relationship between soil matric potential and the normalized temperature rise measured by the HDU. This relationship is general for all the sensors, and hence only a selected few sensors need be used to develop this relationship.

Normalization: Much of the HDU sensor-to-sensor variation is due to variation in the heater-ceramic contact. If the same heating method and heating time is used for each HDU sensor, then the variation

between sensors can be removed by normalizing the measurements. A normalization procedure of Flint et al. (2002), described by Eq. (3.6), was used to calculate a dimensionless temperature rise. These procedures are summarized in Appendix A. The HDU temperature-rise measurement under dry conditions (ΔT_d) was made after the HDU had been placed over oven-dried desiccant in a sealed container for a length of time (approximately 24 hours). For the HDU temperature-rise measurement under water-saturated conditions (ΔT_w), the sensor was submerged in water for 24 to 48 hours and then removed before the HDU measurement. Flint et al. (2002) report that this method of saturating the HDU is sufficient for conditions that will remain drier then -0.1 bar, which are the expected field conditions for this project. All readings were taken with a constant line-heat source current of 50 mA and measurement times of 1 s and 30 s after HDU heating was initiated. Table 4.2 summarizes the normalization results.

Table 4.2. HDU Temperature Rise Under Dry (ΔT_d) and Wet (ΔT_w) Conditions

HDU NO.	**250-1**	**250-2**	**250-3**	**250-4**	**250-5**
Sensor Serial #	11251	11254	11256	11259	11252
ΔT_d (°C)	2.80	2.75	2.59	2.79	2.71
ΔT_w (°C)	0.79	0.80	0.79	0.83	0.80
HDU NO.	**250-6**	**250-7**	**250-8**	**250-9**	**250-10**
Sensor Serial #	11255	11257	11258	11250	11253
ΔT_d (°C)	2.85	2.65	2.68	2.75	2.59
ΔT_w (°C)	0.83	0.82	0.80	0.82	0.78
HDU NO.	**275-1**	**275-2**	**275-3**	**275-4**	**275-5**
Sensor Serial #	11269	11262	11265	11260	11266
ΔT_d (°C)	2.53	2.87	2.82	2.64	2.79
ΔT_w (°C)	0.81	0.84	0.83	0.82	0.79
HDU NO.	**275-6**	**275-7**	**275-8**	**275-9**	**275-10**
Sensor Serial #	11263	11261	11268	11267	11264
ΔT_d (°C)	2.66	2.74	2.79	2.62	2.75
ΔT_w (°C)	0.82	0.84	0.82	0.79	0.84

Calibration: The HDUs were calibrated in the laboratory across the range of expected field soil-water pressures using the procedures described in Appendix A. The calibration was performed using a bucket packed with Hanford's Warden silt loam and containing six HDUs and two tensiometers with pressure transducers for independent matric potential measurements (Figure 4.3). Warden silt loam was used because its water-retention characteristics allow for creating soil-water matric potential over the desired range. HDU calibration is independent of soil texture, permitting the use of Warden silt loam without introducing error into the calibration.

The appropriate amount of soil and water was mixed together to attain the desired water content and hence desired matric potential. Uniform mixing of the soil and water was achieved before packing the soil in the bucket. During packing of the soil, the HDUs and tensiometers were added to the bucket, and soil was packed around the instruments. After packing the bucket, the surface was covered to reduce evaporation. The HDUs and tensiometer pressure transducers were controlled by a single datalogger. The HDU measurements were taken continuously for at least 24 hrs or until steady-state conditions were achieved, as indicated by HDU and tensiometer measurements. HDU readings were taken with a 50 mA current applied to the heating element for 30 seconds. After the measurement set was completed, the procedure was repeated for a different water content (matric potential).

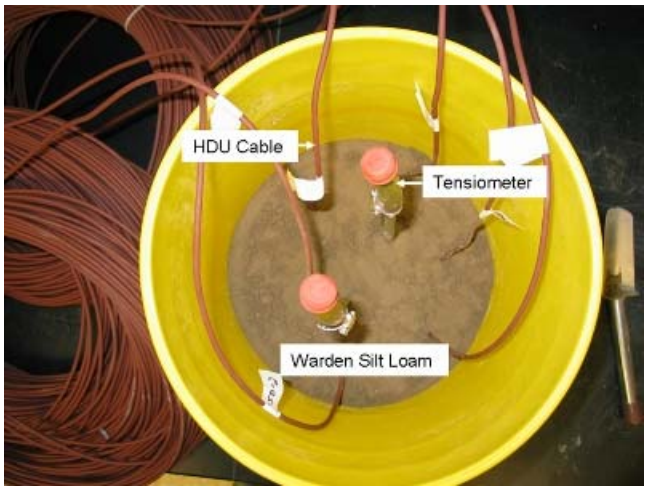

Figure 4.3. Six HDUs and Two Tensiometers Packed in Warden Silt Loam for Calibration of the HDUs. Tensiometer pressure transducers are not present in this figure.

Using the normalized HDU temperature rise and tensiometer readings under steady-state soil conditions, a calibration was developed by fitting a calibration curve to the paired matric potential and normalized HDU data points. Figure 4.4 shows the paired data points and developed relationship between matric potential, ψ (m of water) and normalized HDU response, $S_{\Delta T}$. The dataset is best fit using a second-order polynomial equation described by:

$$\psi = 12.388 \times S_{\Delta T}^2 - 3.9697 \times S_{\Delta T} - 6.2548 \text{ , } r^2 = 0.9689 \quad (4.2)$$

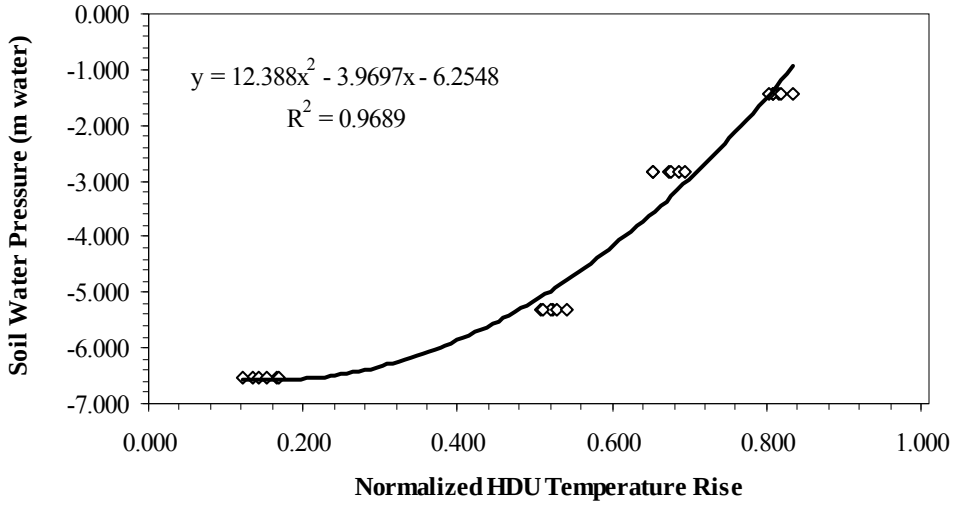

Figure 4.4. HDU Calibration Data Points and Calibration Relationship

4.4 Drain Gauge

The manufacturer's quality-control requirements state that each drain gauge is manufactured to dose at 31 mL ±10%.[(a)] This represents 1 mm of drainage for the 310-cm^2 sampling area of the drain gauge. In addition, drainage resolution of less than 1 mm can be attained by measuring the volume of water in the siphon chamber. A calibration relating volume of water in the chamber, V (cm^3), to the water-depth sensor output, WD (mV), is provided by the manufacture as (Decagon Devices, Inc. 2006):

$$V = 0.33 \times WD^2 - 9.8 \tag{4.3}$$

Both calibrations will be used to convert drain-gauge output to drainage. A drain-gauge dose will be considered 31 mL drainage, and volumes less than 31 mL will use the relationship in Eq. (4.3) to compute drainage water residing in the siphon chamber.

Before installing the drain gauges in the field, each drain gauge was tested to verify that it was functioning. Testing was achieved by slowly applying a known volume of water to the drain-gauge calibration line using a graduated 60-mL syringe while monitoring the gauge for dose events. The volume of water applied for each dose was recorded and compared to the manufacturer's stated calibration (31 mL per dose). Table 4.3 presents results from the tests. Due to the empty volume of the calibration line and the resolution of the syringe (0.5 mL), the differences between calibrated dosing volume and applied liquid were no more than 1.0 mL, which is less than the manufacturer's suggested measurement error of ±10%. The results support that the drain gauges were functioning before installation.

Table 4.3. Drain-Gauge-Function Verification Results

(a) Decagon Devices, Inc., Personal communication.

Test	Volume applied per dose (mL)	
	Gauge 1	Gauge 2
1	31.0	30.5
2	31.0	31.0
3	30.0	31.0

4.5 Temperature Probe

The temperature probes come from the manufacturer already calibrated and do not require a field calibration. Two different CSI models, Model 107 and Model 109, of temperature probes are used. The Model 107 temperature probe is used as a reference temperature probe and is located within the enclosure boxes housing the dataloggers that control the instrument inside the T tank farm. The Model 107 temperature probe is described by a fifth-order polynomial equation relating thermistor resistance, Rs (Ohms), to temperature, T (°C) by (Campbell Scientific Inc. 2004),

$$T = C_0 + C_1 Rs + C_2 Rs^2 + C_3 Rs^3 + C_4 Rs^4 + C_5 Rs^5 \tag{4.4}$$

where C_0 = -53.4601
C_1 = 90.807
C_2 = -83.257
C_3 = 52.283
C_4 = -16.723
C_5 = 2.211

The temperature sensor used as part of the meteorological station is a Model 109 temperature probe. This temperatures sensor relates thermistor resistance to temperature using the relationship (Campbell Scientific Inc. 2004),

$$T = \left\{ \frac{1}{A + B\ln(Rs) + C\left[\ln(Rs)\right]^3} \right\} - 273.15 \tag{4.5}$$

where A is 1.129241×10-3, B is 2.341077×10^{-4}, and C is 8.775468×10^{-8}.

4.6 Rain Gauge

The rain gauge is factory calibrated and does not require a field calibration. The calibration produces an equivalent height of water of 0.254 mm per tip. Before field installation, the functionality of the rain gauge was confirmed by applying a known volume of water to the rain gauge with a graduated 60-mL syringe while monitoring for tips. The volume of water applied for each tip was compared to the manufacturer's calibration (8.3 mL per tip) to see that there was general agreement between the two. Table 4.4 presents results from this analysis. Differences between the calibrated tipping volume and the volume of water applied were no more than the resolution volume of the syringe (0.5 mL). The results confirm that the rain gauge is functioning.

Table 4.4. Rain-Gauge-Function Verification Results

Test	Volume applied per tip (mL)
1	8.5
2	8.5
3	8.5

5.0 Instrument Layout and Installation

During August and September of 2006, two nests of vadose zone monitoring instruments were installed within T Tank Farm, and a meteorological station was installed outside of the tank farm. Each of the two instrument nests within the tank farm included its own datalogger as did the meteorological station outside the farm. This section updates the discussion in the design plan to represent any change and slight modifications to the installation procedure. Adjustments to the locations of two additional nests planned for FY 2007 are also presented.

5.1 Selection of Monitoring Locations

The instruments are installed both under the interim surface barrier and outside of the surface barrier for purposes of monitoring surface-barrier impacts on the subsurface water regime. Three-dimensional simulations presented in Section 2 and two-dimensional simulations[(a)] suggest that the measurable changes in subsurface conditions 3 years after surface barrier placement will primarily be contained in the top 15 m of sediment. Longer time periods are required before measurable changes propagate to deeper depths. As such, a combination of shallow and deep instrument placement is incorporated into the monitoring design.

Nest placement is guided by three primary factors: 1) the capability to distinguish the differences in soil-water regimes in the regions with and without a surface barrier, 2) the capability to investigate edge effects, and 3) the locations of existing underground utilities (e.g., pipelines, electrical conduits) or structures and the geometry of the planned interim surface barrier. The nest placement should provide the greatest opportunity for monitoring instruments to detect changing subsurface soil-water conditions. For example, in the region with a surface barrier, the water content of the soil close to or between tanks is expected to have a larger change than the soil far away from the tanks.

Those designing a monitoring system also need to consider that soil attributes may vary in space. This requires that the monitoring of a flow variable should be taken at multiple locations, if possible. There are three options for repetitive measurements: 1) multiple measurements horizontally, 2) multiple measurements vertically, and 3) multiple measurements both horizontally and vertically. Other factors to be considered include the cost constraint for instrument purchase, installation and monitoring, the method of installation, and the depth of a surface barrier that affects the soil-water regime within the time frame of monitoring. The use of options 1) and 3) are more costly than option 2) to achieve similar measurement repetition. Hence, option 2) is used for instrument placement.

Horizontally, the instruments are grouped into four nests (i.e., A, B, C, and D), each of which includes a neutron access tube, a capacitance probe, and an HDU. Nest A is placed in the area without a cover and serves as a control. It needs to be at least 5 m away from the closest edge of the surface cover to prevent measurable impacts from the cover. Nest B is placed at the edge of the surface barrier to monitor the edge effect of the surface barrier on the soil-water regime. Each Nest (A and B) also contains a water-flux meter. Nests C and D are duplicates and are placed inside the covered area; they need be at least 5 m from the closest edge of the surface barrier and between two or more tanks where the largest change of soil-water content, and hence water flux, is expected after the emplacement of the surface barrier.

(a) McMahon, W., 2007, Personal communication.

Vertically, the monitoring depths go to 15-m bgs. Considering that, upon the emplacement of the surface barrier, the changes of soil moisture will be more significant in shallower depths; more intensive and frequent measurement will be taken in small depths.

5.2 Instrument Nest Design

As described above, the design groups instruments and access tubes into four nests, with each nest being composed of a vertical access tube for neutron-moisture-probe measurements, an EnviroSMART capacitance probe, and HDU units. In addition, each Nest (A and B) contains a drain gauge. Figure 5.1 provides a plan view of the existing instrument nest locations (A and B), the prospective location for two additional instrument Nests C and D to be installed in FY 2007, and the probable footprint of the interim surface barrier. After surface-barrier placement, Nest A will continue to provide subsurface conditions outside the surface barrier area. Nest B, at the edge of the surface barrier, will provide subsurface measurements that are aimed to explore the magnitude of surface-barrier edge effects. Nests C and D will serve as a redundant measurement of conditions beneath the interim surface barrier at locations where subsurface hydraulic conditions are anticipated to exhibit the greatest change, as supported by model results. All present and future instrument nests lie within backfill material, except for the lower part of the neutron access tubes, which extend into the undisturbed Hanford formation below the tanks.

Nests A and B were installed in late FY 2006, and monitoring was initiated on September 29, 2006. Figure 5.1 shows the approximate location of each instrument installation. Table 5.1 provides the coordinates of each well using the Washington Coordinate System, NAD83(91) datum. Nests A and B will provide baseline conditions before installing the interim surface barrier, anticipated to occur in the summer of 2007. Nests A and B are installed at a separation distance of approximately 20 m, with Nest A being outside the proposed surface-barrier area, and Nest B being near the edge of the surface barrier. Both nests are approximately 11 m from the nearest tank.

Nests C and D are planned to be installed in FY 2007. Nests C and D will be inside the surface-barrier area, with Nest C being between tank T106 and T109, and Nest D located approximately at the center of the interim surface barrier, between tanks T105, T106, T108, and T109 (Figure 5.1). The instrumentation and configuration of both nests will be identical in design to Nests A and B, except that Nests C and D will not include a drain gauge. The final instrument composition of Nests C and D will be a vertical access tube for neutron-moisture-probe measurements, an EnviroSMART capacitance probe, and HDU units. Table 5.2 summarizes the vertical placement of instrument or measurement points. The sensor serial numbers and/or sensor numbers for the capacitance and HDU sensors are listed in Table 5.3 and Table 5.4, respectively.

In addition to the instrument nests, some of the existing dry wells located in the T Farm may be neutron logged, provided the wells have a favorable completion design. These data may provide information regarding the soil-water condition in the regions that are not monitored by the above-mentioned instrument nests. The following wells appear to be suitable for neutron logging: 50-08-11, 50-05-04, 50-09-01, 50-08-08, 50-11-11, and 50-08-19 (Figure 5.2).

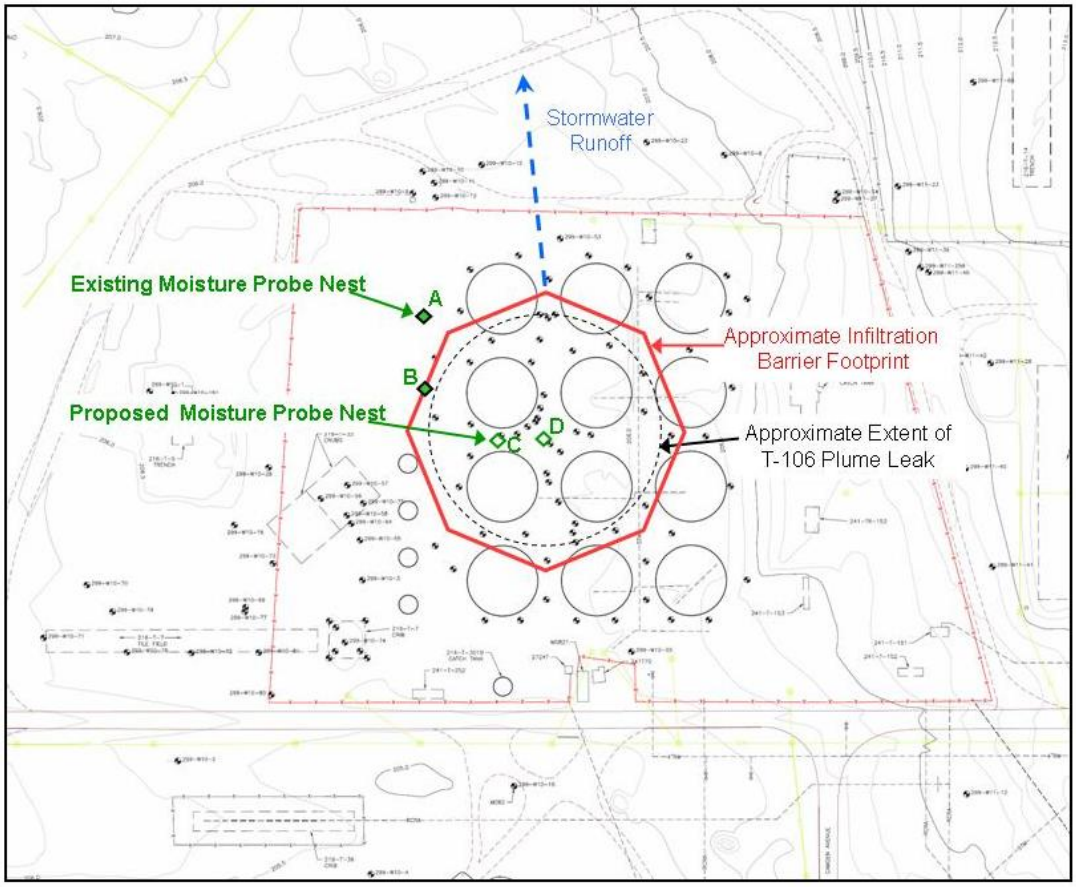

Figure 5.1. Plan View of T Tank Farm with the Approximate Locations of Existing Monitoring Nests A and B, Prospective Monitoring Nests C and D, and Proposed Interim Surface barrier Boundary as Marked by the Octagon

Table 5.1. Vadose Zone Monitoring Driving Boreholes Coordinates Drilled in FY2006 and Associated Installed Instruments

Well Number	Instrument	Coordinates[(a)]	
		Northing (m)	Easting (m)
C5306	Drain Gauge	136762.16	566752.82
C5307	Access Tube	136761.16	566752.82
C5309	HDUs	136760.16	566751.82
C5310	Capacitance Probe	136761.16	566751.82
C5311	Drain Gauge	136739.59	566753.47
C5312	Access Tube	136738.59	566753.47
C5314	HDUs	136737.59	566752.47
C5315	Capacitance Probe	136738.59	566752.47
(a) Washington Coordinate System, NAD83(91) datum			

Table 5.2. Instrument Vertical Placement

Methods	Nest	No. of Sensors/ Measurement Points	Depth of Sensors/ Measurement Points
Capacitance Probe	A, B, C, D	5	0.6, 0.9, 1.3, 1.8, and 2.3 m
Neutron Probe	A, B, C, D	50	from 1 to 50 ft bgs at 1-ft interval
HDU	A, B, C, D	4	1, 2, 5, and 10 m
Drain Gauge	A, B	1	ground surface

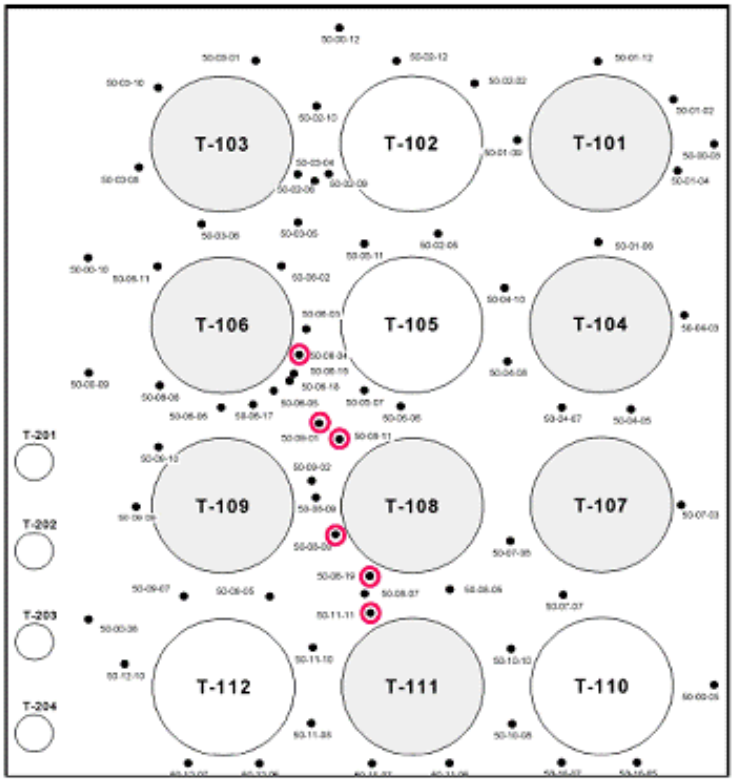

Figure 5.2. Plan View of T Tank Farm with the Dry Wells Expected to Be Suitable for Neutron Moisture Logging Being Marked in Circles

Table 5.3. Serial Numbers of the Capacitance Sensors Installed in Nests A and B

Depth (m)	Nest A	Nest B
0.6	AP06-305	FE06-371
0.9	AP06-310	FE06-372
1.3	AP06-303	FE06-373
1.8	AP06-304	FE06-374
2.3	AP06-309	FE06-375

Table 5.4. Serial Numbers and Sensor Numbers of the HDU Sensors Installed in Nests A and B

Depth (m)	Nest A		Nest B	
	Sensors S/N	Sensor #	Sensors S/N	Sensor #
1	11256	250-3	11261	275-7
2	11257	250-7	11268	275-8
5	11258	250-8	11267	275-9
10	11259	250-4	11263	275-6

5.3 FY 2006 Instrument Installation

In FY 2006, instrument Nests A and B were installed following the placement and methods described below. Instruments were placed in an open driving borehole created by pounding a cone-tipped hollow drive shaft into the ground using a hydraulic hammer. Figure 5.3 shows a typical cone-tipped drive shaft used for driving boreholes. The benefit of using the hydraulic hammer to create a borehole as opposed to drilling is that the hydraulic-hammer technique avoids bringing potentially contaminated soil to the surface. The cone tip on the drive shaft has the capability to be removed once the desired driving depth is reached. This allows instruments to be placed down the borehole through the inside of the drive shaft as the drive shaft is removed from the soil. Likewise, the drive shaft can remain in the soil as a permanent access tube. The diameter of the borehole can be increased or decreased using differing drive-shaft and drive-head diameters.

The following discussion provides specific details of each instrument installation and is adapted from Zhang and Keller (2006) to reflect installation modifications. Both metric and English units of measurement are reported in this section to be consistent with the English units used by the drillers to measure and report depths and instrument-installation details.

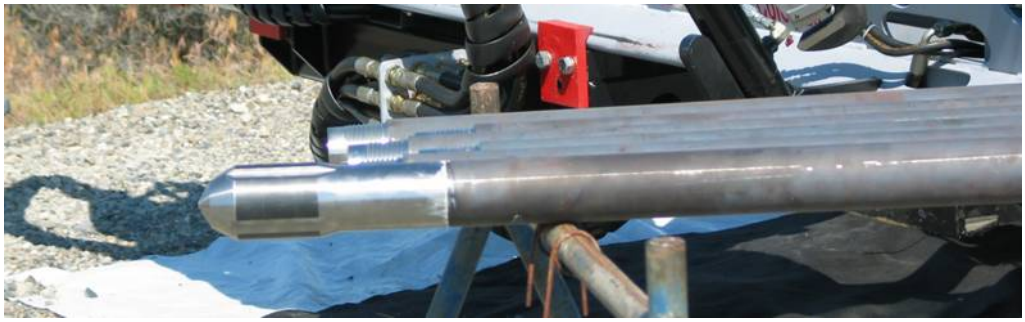

Figure 5.3. Cone-tipped Drive Shaft Used in Conjunction with a Hydraulic Hammer for Creating Driving Boreholes

5.3.1 Neutron-Moisture-Probe Access Tubes

Each neutron-probe access tube was installed using the basic function of the hydraulic hammer. A steel access tube 4.45 cm ID, 6.35 cm OD (1.75 inch ID, 2.5 inch OD) was driven vertically by the hydraulic hammer to a depth of 15.24 m (50 ft). A cap on the access tube is used to prevent precipitation from

entering the access tube. Figure 5.5 shows the diagram of the installed neutron-probe access tubes and installation procedures.

5.3.2 EnviroSMART Capacitance Probe

To allow the capacitance probe access tube with a 5.65 cm (2.22 inch OD) to be placed into the ground through the drive shaft, an 8.48 cm (3.34 inch) ID drive rod was used. The OD of this drive shaft was 10.16 cm (4.00 inches), resulting in an annulus of 4.51 cm (1.78 inches). At both instrument nests, the drive rod was driven to a depth of approximately 3.50 m (11.50 ft). Once the target depth was reached, the drive cone was detached from the shaft, and the cone was isolated from the capacitance probe by surrounding it with 20/40 clean sand until the borehole depth was approximately 2.83 m (9.28 ft). The EnviroSMART PVC access tube was then placed at depth through the drive rod, with the top of the probe being approximately 0.30 m (0.98 ft) below ground surface. As the drive rod was extracted, 20/40 clean sand was packed in the annulus surrounding the polyvinyl chloride (PVC) access tube.

The drive-rod diameter was selected to create as small of an annulus as possible. However, the annulus size still required packing the 20/40 sand around the access tube to eliminate any air gaps around the access tube. Keeping the size of the annulus to a minimum was important so that the measured moisture content of the capacitance probe is not heavily skewed by the moisture content of the packing material. The manufacturer of the probe states that 99% of the probe reading is taken within a 10-cm radius from the outside of the capacitance-probe access tube. Given that the radial thickness of the 20/40 clean sand packed in the annulus is 4.51 cm (1.78 inches), this suggests that approximately 45% of the capacitance-probe reading is interrogating the 20/40 clean-sand material. While the sand pack will skew absolute soil-water-content values, relative trends over depth and time will still be valuable.

Figure 5.4. Capacitance Probe Cap and Protective Casing at Instrument Nest B Before Filling With Tank Farm Surface Material

Near the top of the borehole, an approximately 5 cm (1.97 inches) thick layer of hydrated bentonite crumbles was added to the annulus to reduce the potential for preferential flow through the 20/40 sand pack material. After the PVC access tube and packing material was emplaced, accumulated soil and dust within the access tube was removed, and the sensors were placed within the access tube as was desiccant. The access tube was then capped and sealed with a water-tight and weather-resistant sealant.

To protect the probe from surface traffic, a 25.4-cm (10-inch) diameter steel casing was placed around the access tube, extending from the surface to a depth of 0.30 m (1 ft). The casing was then filled with soil material from the tank farm surface. Figure 5.4 shows the capacitance probe cap and protective casing before filling the casing with the tank-farm surface material, while Figure 5.7 shows a diagram of the installed capacitance probe access tubes and installation procedures.

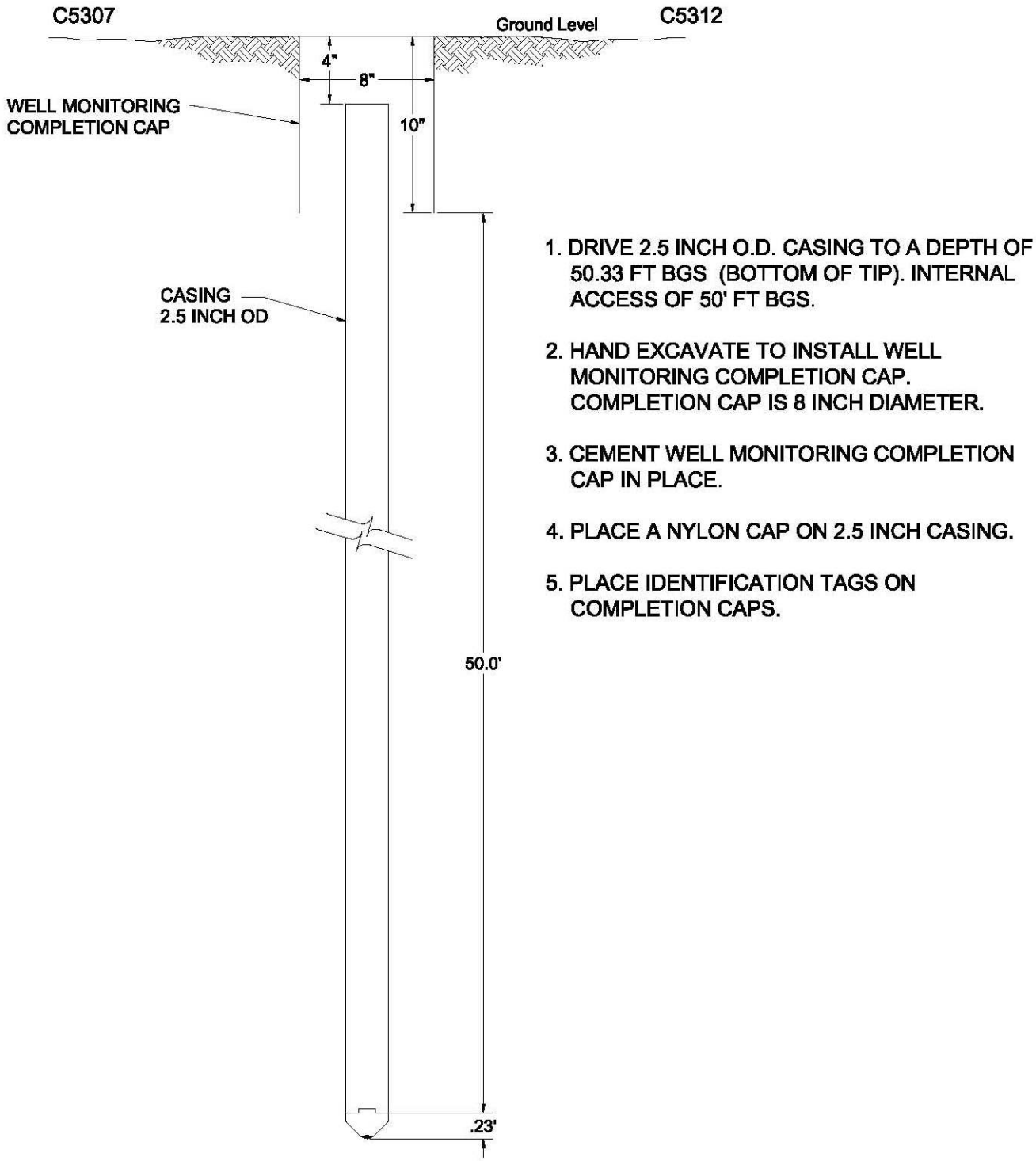

Figure 5.5. Diagram of the Installed Neutron Probe Access Tubes and Installation Procedures (after CHG 2006)

5.3.3 Heat-Dissipation Units

HDUs were installed within a borehole created by driving a 4.45-cm-ID, 6.35-cm-OD (1.75–inch-ID, 2.5–inch-OD) steel drive shaft and drive head set to a depth of 10.97 m (36.0 ft) using the hydraulic hammer. Figure 5.8 provides a representation of the packing material and instrument layering scheme for installing the HDUs within the borehole. Once the drive shaft was at depth, the drive cone was disconnected from the drive shaft, and as the rod was removed, 20/40 clean sand was added to bring the level to approximately 10.0 cm (3.9 inches) below the bottom HDU depth of 10.0 m (32.8 ft). The HDU and silica flour were added for a total of 20.0-cm (7.9-inches) thickness of silica flour. Silica flour was packed around the HDU to supply optimum contact between the sensor and surrounding soil material. The silica flour was moistened slightly before adding to the borehole to improve packing of the flour and to reduce HDU equilibration time with the surrounding sediment. Approximately 20.0 cm (7.9 inches) of 20/40 sand was then added on top of the silica flour, followed by hydrated bentonite crumbles to a depth of approximately 30.0 cm (11.8 inches) below the next instrument depth of 5.0 m (16.4 ft). 20/40 sand was added to bring the level to approximately 10.0 cm (3.9 inches) below the instrument depth. The next HDU and silica flour was then added as was done with the previous HDU. This sequence was repeated until all HDUs were installed. After the last HDU was installed, 20.0 cm (7.9 inches) of 20/40 clean sand was added before the borehole was completed to the surface with hydrated bentonite crumbles. A representation of this packing scheme is presented in Figure 5.8. To protect wiring and instruments from vehicle traffic, a 20.3-cm (8.0-inches) diameter steel casing was placed over the borehole to a depth extending 0.30 m (1.0 ft) below the soil surface, and the casing was capped. Figure 5.6 shows the HDU installation before placing a cap on the protective casing. Note the HDU cabling that runs to the datalogger.

Figure 5.6. Protective Casing Over the HDU Location at Instrument Nest B

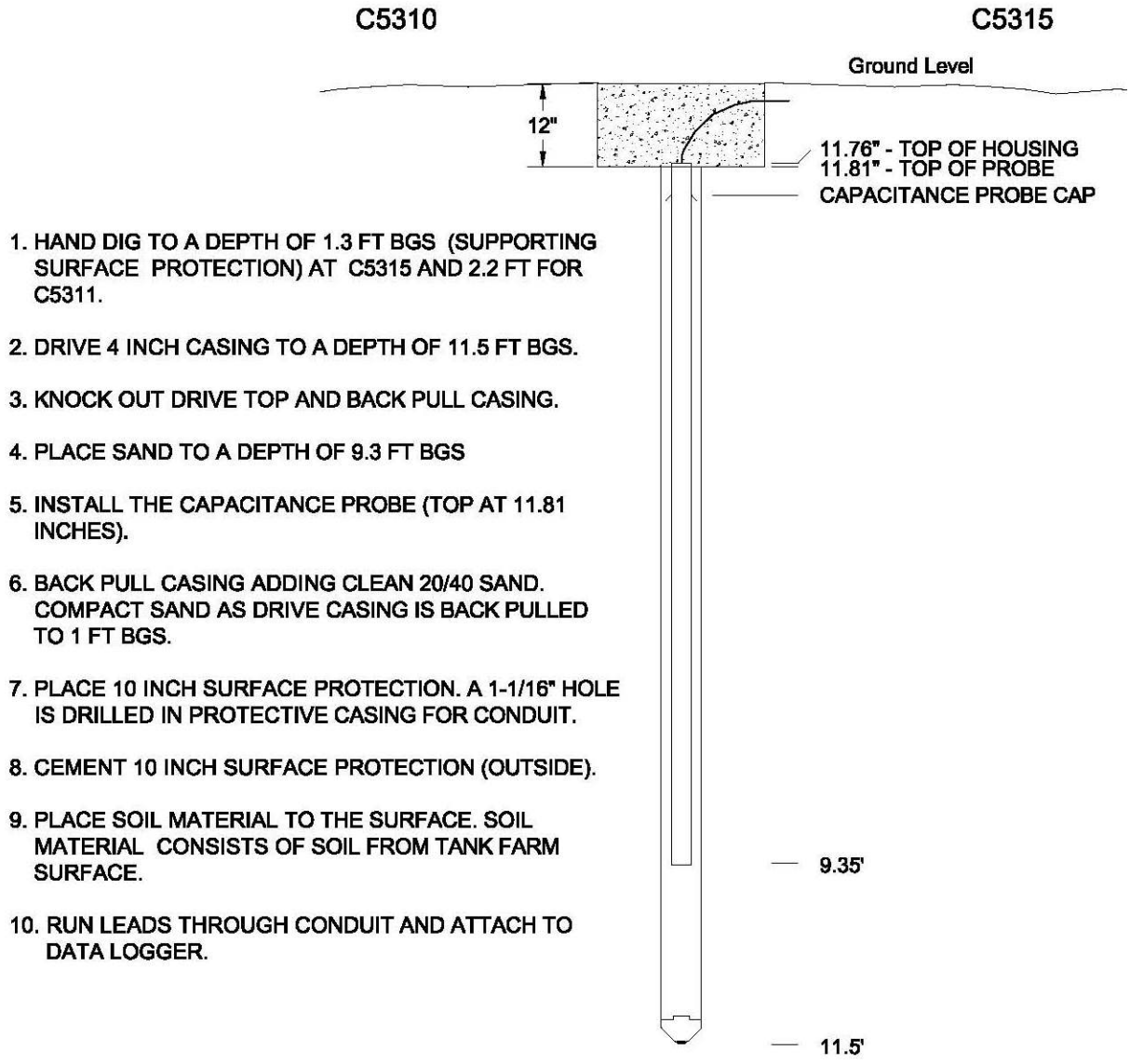

Figure 5.7. Diagram of the Installed Capacitance Probe Access Tubes and Installation Procedures (after CHG 2006)

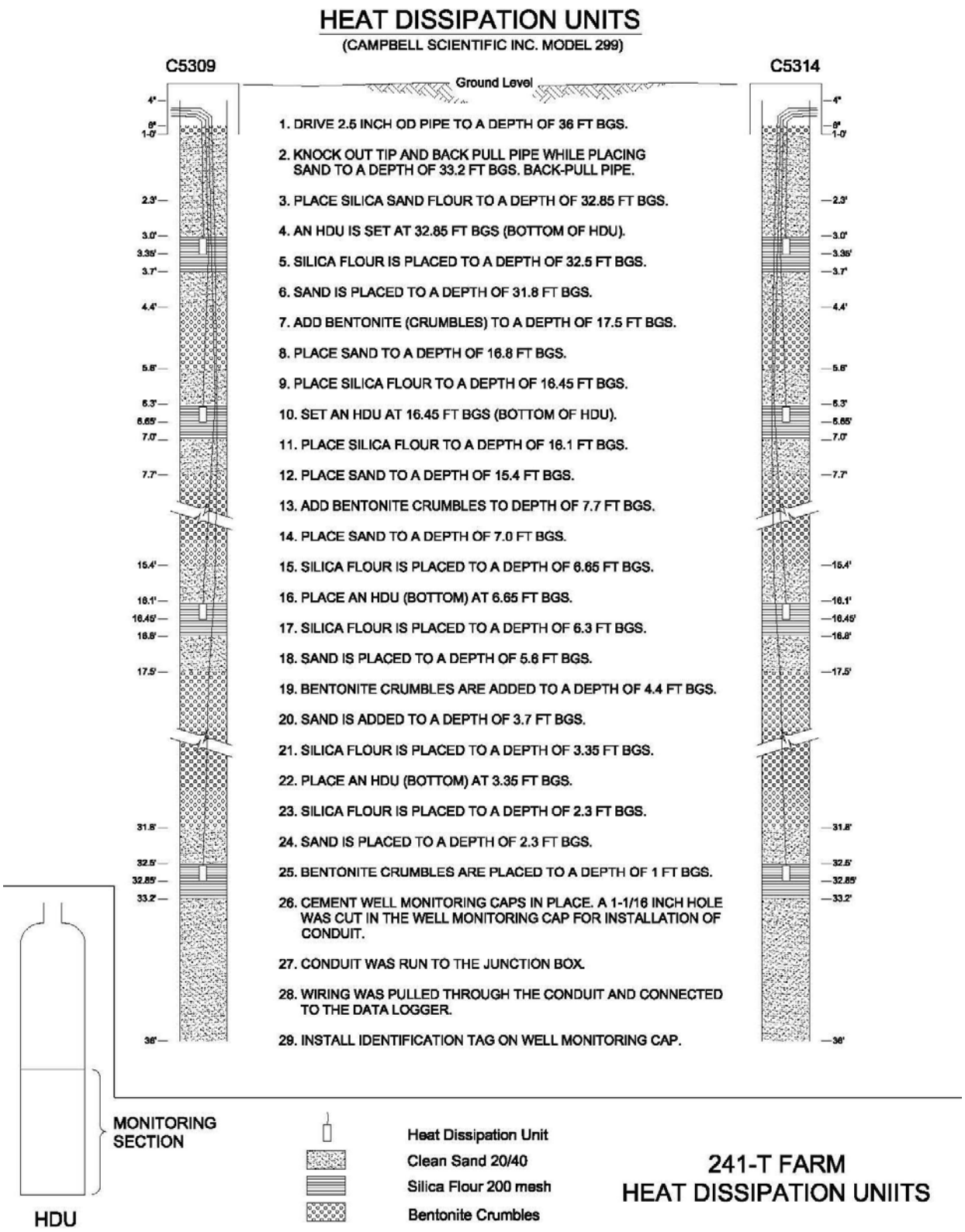

Figure 5.8. HDU Installation and Packing Material Layering Scheme (after CHG 2006)

5.3.4 Drain Gauge

The drain gauge has a 20.3-cm (8.0-inch) OD divergence control tube that is 0.67 m (2.2 feet) in length, requiring a hole of this diameter to be created from the surface to a depth of 0.67 m (2.2 feet). An auger was employed to create a sufficiently large diameter hole to allow placement of the divergence control tube. To preserve the hole while auguring, a 25.4-cm (10-inch) diameter casing was advanced as the auguring proceeded. The sediment removed during auguring was set aside to be used later to pack the divergence control tube. After auguring to the correct depth, a 4.45-cm-ID, 6.35-cm-OD (1.75-inch-ID, 2.5-inch-OD) drive shaft and drive-head combination was pushed, starting from the base of the augured hole to a depth of approximately 1.2 m (4 ft) past the base of the auger hole. The hole was pushed multiple times until it maintained its structure when the drive shaft was removed. Gravel was added to the bottom of the smaller diameter borehole until approximately 0.30-m (1-ft) depth of gravel was present. The gravel allows for unabated movement of the dosing water away from the drain gauge. The wick section of the drain gauge was then placed inside the smaller diameter borehole with the top plate of the

Figure 5.9. Instrument Nest B Drain Gauge (smaller diameter tube) and Protective Casing (larger diameter tube). Also shown are the solution sampling line (blue tube) and drain gauge calibration and testing line (clear tube).

wick section resting on the bottom of the auger hole. A 2-cm-thick (0.79-inches) layer of manufacturer-provided diatomaceous earth was placed on top of the fiberglass fabric that covers the top plate to enhance contact between the soil in the divergence control tube and the fiberglass wick. The divergence control tube was then securely placed on the top plate of the wick section and packed with the augured out soil. The drain gauges were placed at both nests so that the divergence control tube and steel casing terminated at ground surface, with the steel casing remaining to provide an added level of protection for the drain gauge. Figure 5.9 shows the drain gauge at instrument Nest B before the surface material was

packed. In this figure, the drain gauge is the smaller diameter tube, and the larger diameter tube is the protective casing. The clear tube coming from the drain gauge is a calibration tube that allows for calibration of the unit after it has been installed and allows the functionality of the unit to be checked. The blue tube can be used to extract a solution sample from the unit if desired. Figure 5.10 shows a diagram of the installed drainage gauges and installation procedures.

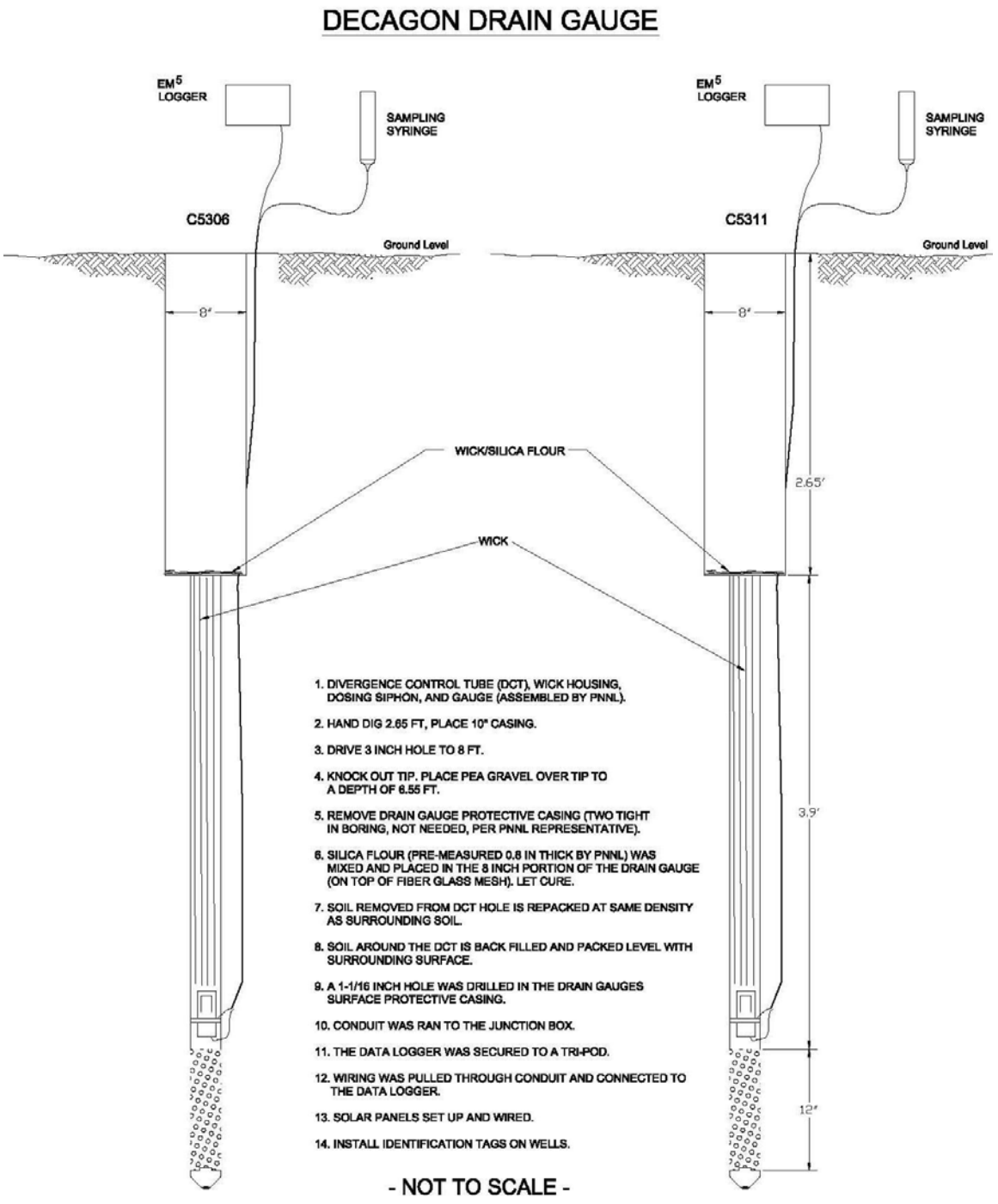

Figure 5.10. Diagram of the Installed Drainage Gauges and Installation Procedures (after CHG 2006)

5.3.5 Datalogger and Wiring

Each instrument nest within the tank farm will be connected to a dedicated datalogger adjacent to the instrument nest. Wiring from each instrument is run through buried conduit that terminates at a transfer box. The wiring then runs from the transfer box to the datalogger enclosure box through a single line of conduit. The datalogger is installed in a weather-tight enclosure containing desiccant bags to reduce moisture inside the box. The enclosure and transfer box is attached to a 6-foot-tall galvanized steel tripod that is securely anchored using 12-inch-long rebar ground stakes. The tripod is grounded to a 5-inch grounding rod.

The datalogger and peripherals are powered by a 12-volt rechargeable battery, which is charged by a solar panel attached to the tripod. The battery is placed within the enclosure. Data from the datalogger are transmitted remotely by a 900-MHz spread spectrum radio to a receiving computer located outside of the tank farm. Figure 5.11 shows the datalogger enclosure and other infrastructure associated with the datalogger station controlling instrument Nest B. Each instrument nest is surrounded by T-posts and rope to deter vehicle traffic. Figure 5.13 shows the wiring diagram for the instrument nests inside the T tank farm. The wiring for Nests A and B are identical.

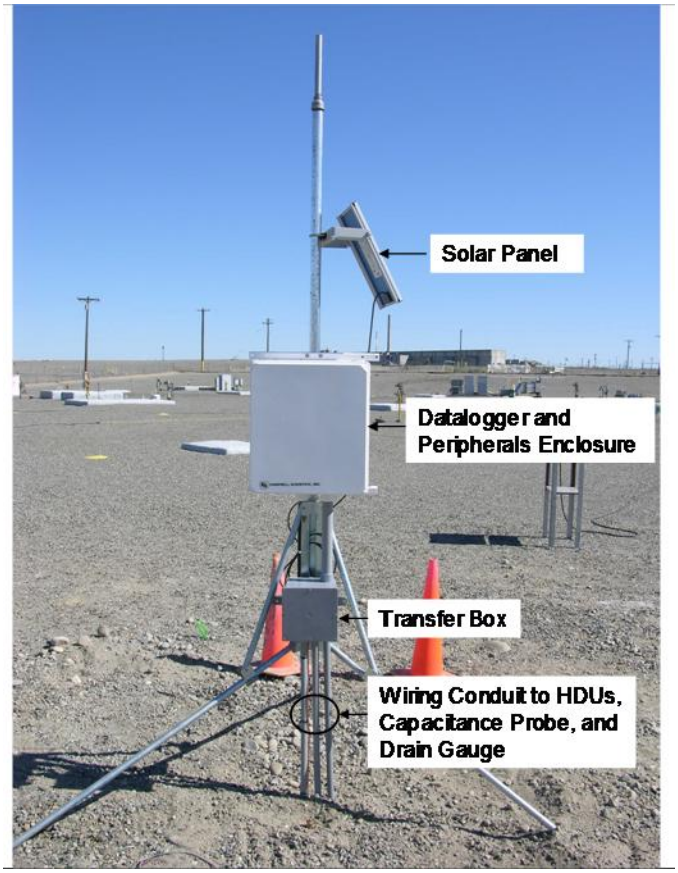

Figure 5.11. Instrument Nest B Tri-pod with Attached Solar Panel, Datalogger Enclosure, and Transfer Box

5.3.6 Meteorological Station

The meteorological station was installed along the north fence line, just outside of the T tank farm. The datalogger and meteorological instruments are mounted on a 6-foot-tall galvanized steel tripod that is securely anchored using 12-inch-long rebar ground stakes. The datalogger controlling the instruments is placed inside a weather-resistant enclosure. The datalogger is powered by a 12-volt rechargeable battery that is charged by a solar panel attached to the tripod. The battery is placed within the enclosure. Data from the datalogger are transmitted remotely by a 900-MHz spread spectrum radio to a receiving computer. Figure 5.12 shows the meteorological station instruments and control components. A smaller version of the wiring diagram for T Tank Farm Instrument Nests and the meteorological station (CHG 2006) is presented in Figure 5.13.

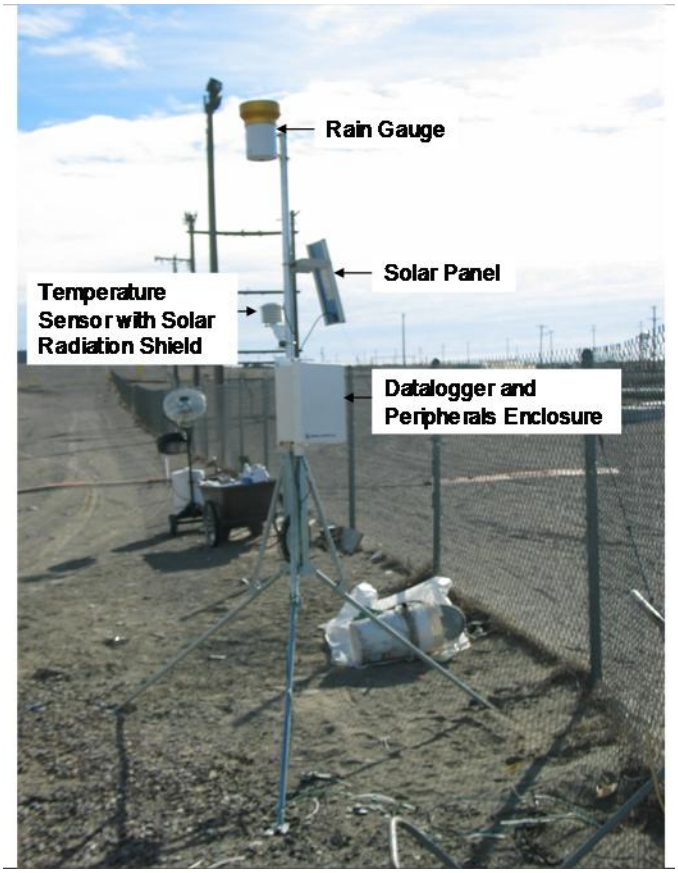

Figure 5.12. Meteorological Station Tri-pod with Attached Solar Panel, Datalogger Enclosure, Rain Gauge, and Temperature Sensor

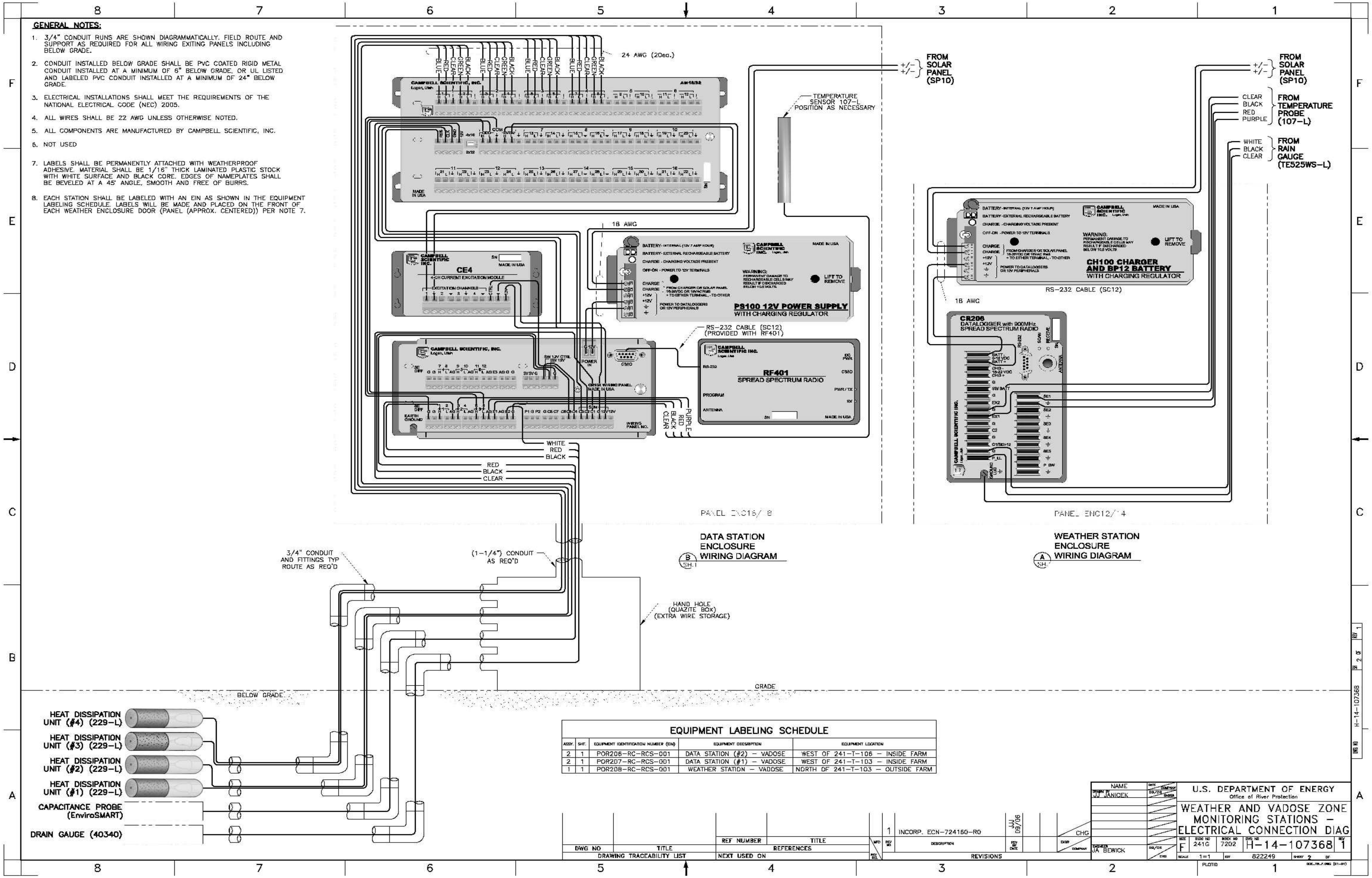

Figure 5.13. Wiring Diagram for T Tank Farm Instrument Nests and Meteorological Station (after CHG 2006)

6.0 Vadose Zone Monitoring Plan

A monitoring plan is presented that uses the monitoring design described in Section 5.0 that will be used to document vadose zone response to the placement of an interim surface barrier in the T tank farm. The monitoring plan employs the measurement of subsurface hydraulic conditions directly beneath and outside of the interim surface barrier as well as meteorological conditions. This section details aspects of the monitoring plan, including:

- the source, method, frequency, and schedule of data collection
- data reduction, validation, organization, and analysis
- instrument performance and vadose zone response indicators
- contingencies given instrument failure
- data reporting.

6.1 Measurement Procedures and Frequencies

This section describes the standard procedures to be used for collecting data under the monitoring design described in Section 5.0 as well as the measurement schedule. Table 6.1 summarizes the six variables to be monitored, the monitoring methods, and the approximate monitoring frequency. The monitoring procedures and frequency may be adjusted as more experience is gained.

Table 6.1. Data Collection Method[(a)] and Approximate Frequency Under Normal Working Condition

Monitoring Component	Monitoring Method	Monitoring Frequency
Soil-Water Content	Neutron Moisture Probe	Quarterly
Soil-Water Content	Capacitance Probe	Every 6 hours
Soil-Water Pressure	Heat Dissipation Unit	Every 6 hours
Soil Temperature	Heat Dissipation Unit	Every 6 hours
Soil-Water Drainage	Drain Gauge	Hourly
Air Temperature	Thermister	Hourly
Precipitation	Rain Gauge	Hourly

(a) All measurements except neutron probe will be controlled by dataloggers and taken automatically. The data will be transmitted to the project server on a weekly basis.

Neutron-moisture-probe measurements will be performed manually. The measurements will initially be made about every 3 months, but may vary according to the needs and the variation of soil-water content. Following the neutron-probe-measurement procedure documented in CHG (Ross 2007), profile measurements will be made at 1-foot intervals to the depths of the access tubes.

The datalogger will control the probe and store the measurement data of moisture content from capacitance sensors, soil-water pressure and soil temperature from HDUs, drainage from the drain gauges, precipitation from the rain gauge, and air temperature from the thermister. Soil-moisture-content measurements made with the capacitance probe and HDU measurements to monitor soil-water pressure

and soil temperature will be taken once or more every 6 hours. At this measurement frequency, a fully charged battery can last for approximately 30 days without being charged by the solar panel. A concern for a more frequent measurement is that the HDU may drain too much power from the battery, especially in the winter months when cloud cover reduces the capability of the solar panel to charge the battery. Air temperature in the meteorological station will be measured every hour or shorter considering that air temperature changes quicker than other variables. Both precipitation and water flux will be measured continuously, but the former is reported hourly. The data will be transmitted to the project server on a weekly basis.

6.2 Data Management

Given the variety and volume of data to be collected, it is critical that the data generated under the monitoring plan be consistently managed in a high-quality format and continuously validated. Doing so allows for reliable routine review and assessment of the functionality of the sensors. The following sections discuss the review and archival of raw data collected by the instrument/datalogger, the reduction of the data into meaningful parameter quantities, and data validation.

6.2.1 Raw Data Review and Archival

The data from the dataloggers are treated as raw data. These data will be reviewed before they are archived in a central server. In the case when the data are not complete, the data will be re-retrieved from the dataloggers. The data from the dataloggers will be in ASCII format. The files from the instrument nests will have the same or similar format as described below. However, the file formats are subject to change if needed. The actual format of each data file will be described in a data-configuration-information file, which is prepared when a data file is archived.

- The file contains multiple rows of comma-delimited data measured at different times. The comma-delimited values correspond to the following variables sequentially:
  - Columns 1 to 5: Array No., Year, Day of year, Hour/Min, Seconds
  - Columns 6 to 7: Battery voltage (V), Reference temperature (°C)
  - Columns 8 to 11: HDU initial temperature at 1, 2, 5, 10 m bgs (°C)
  - Columns 12 to 15: Temperature difference between 1 sec and 30 sec for HDUs at 1, 2, 5, 10 m bgs (°C)
  - Columns 16 to 20: Capacitance-probe scaled frequency from sensors at 0.6, 0.9, 1.3, 1.8, and 2.3 m bgs
  - Columns 21 to 25: Capacitance probe soil-moisture content from sensors at 0.6, 0.9, 1.3, 1.8, and 2.3 m bgs (volume %)
  - Columns 26 and 27: Number of drain gauge doses and siphon water level (mV)
- The file from the Meteorological Station contains the comma-delimited values corresponding to the following variables sequentially:
  - Column 1: Date/Time
  - Column 2: Record number
  - Column 3: Battery voltage (V)
  - Column 4: Rain gauge (inch)

- Column 5: Air temperature (deg C).

Note that in case measurement frequencies do not match, the same value for the less-frequent measurements will be repeated to keep the same data format as described above. Should there be additional data output, they will be added after the above mentioned data items in a row.

6.2.2 Data Reduction and Organization

All monitoring data to be collected require a calibration to relate the measured instrument output of an electric signal to a meaningful parameter value. In the case a calibration is not available for the neutron probe, relative values will be derived. In instances where the instrument calibration is stable and will not change with time, the datalogger will perform the calculation, and the calculated value will be included in the data file. For other instruments, the application of the calibration equation will be done through post processing of the data file. Applying the calibration during post processing allows for the datalogger data file to remain consistent in terms of output fields and to derive the values in the data file.

Data collected under the monitoring plan will be managed in a centralized electronic database repository. The database will be backed up daily using an automated back-up routine. Except for the neutron moisture probe data, data will be automatically or manually downloaded from the datalogger to the project server using a combination of radio-frequency telemetry and/or telephone communication. Data are to be downloaded from the datalogger to the project server approximately once a week. Neutron-moisture-probe data will be copied to the project server after measurements are made. Templates (e.g., using MathCad, EXCEL) will be used to apply the specific instrument calibration and to produce time series plots of the data. The processed data and plots will be stored in the project server. Figure 6.1 presents a flow diagram describing the monitoring components, instrumentation, and data collection and management.

6.2.3 Data Validation

Monitoring data that have been copied to the central server will be screened regularly for anomalies by comparing recent data to historical data and using performance indicators defined in the next section. Anomalous data will be flagged and further investigated following procedures identified in the data-analysis section. If the data are proven to be erroneous, the data will either be corrected, if possible, or noted as suspect. Generally, the data will be validated approximately quarterly, but the validation frequency may be adjusted as more experience is gained.

6.3 Data Analysis

Data analysis will be consistent with the purpose, goals, and objectives of the interim-surface-barrier monitoring plan to assess the performance of the interim barrier. Data represent measurements at selected monitoring locations at selected times and include soil-water content, soil-water pressure, soil temperature, soil drainage, and meteorological conditions.

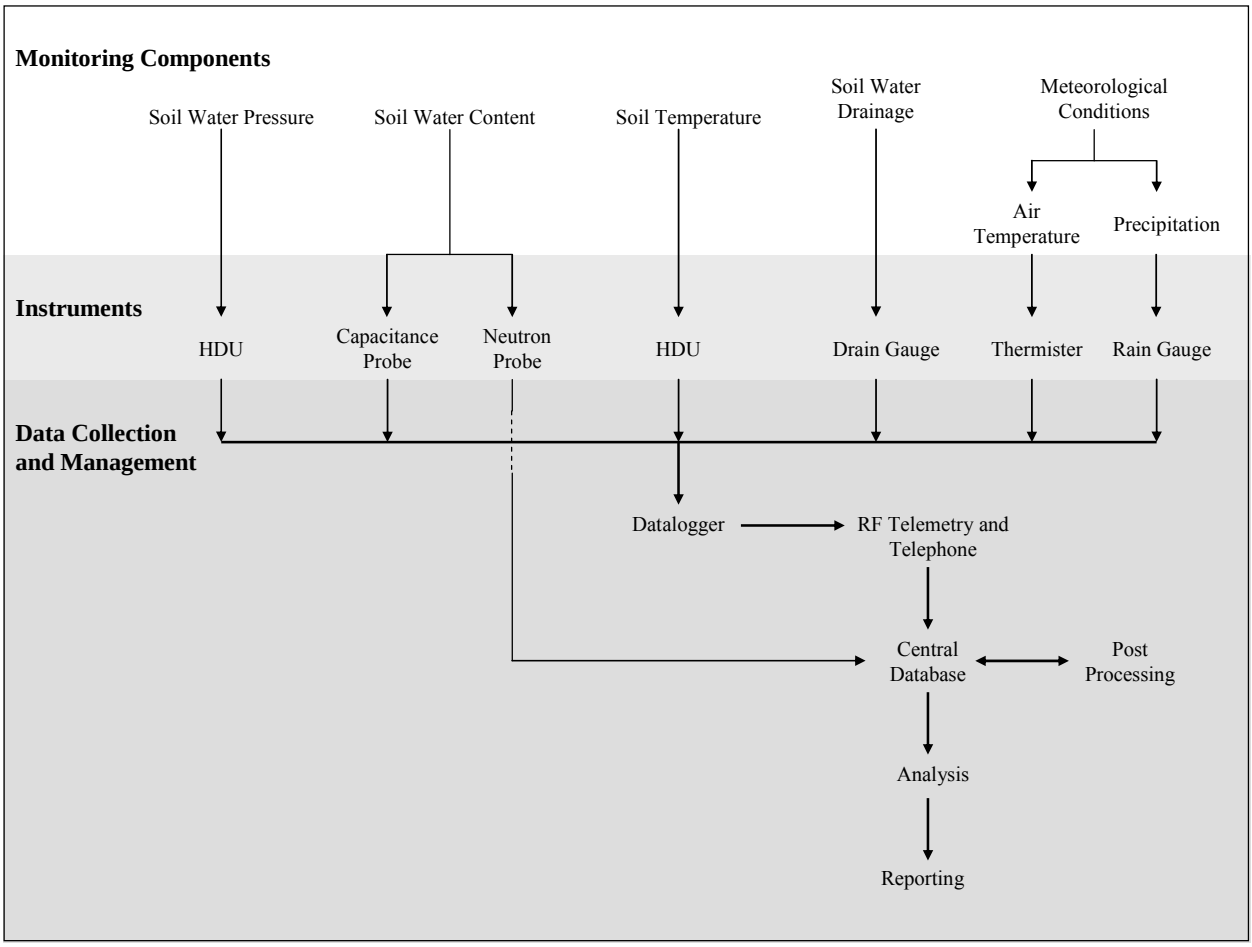

Figure 6.1. Monitoring Components, Instrumentation, and Data Collection and Management Flow Diagram

This section provides a general discussion of the analysis and assessment of the measurement data, with an emphasis on instrument performance indicators and vadose zone response indicators. If necessary to better represent subsurface conditions, performance indicators may be revised in the future in response to measured background data. The data will be summarized in reports that will include tabular and graphical summaries of the monitoring data. The reports will identify any potentially significant anomalies that may require attention.

6.3.1 Instrument Performance Indicators and Contingencies

Performance indicators to evaluate instrument functionality are presented. Unmet performance indicators may be a result of real unexpected subsurface conditions, data-transmittal error, post-processing error, or instrument malfunction. In the case of unexpected subsurface conditions, the performance indicators may require adjustment after baseline data are collected. For instances when performance indicators are not met, suggested troubleshooting methods are presented as are contingencies. Table 6.2 summarizes the performance indicators outlined in this section.

Table 6.2. Instrument Performance Indicators

Monitoring Method	Monitoring Component	Performance Indicator
Neutron Moisture Probe	Soil-Water Content (θ_v)	$0.75 \leq SDR \leq 1.25$
		$SC = \pm 0.98 \times \sqrt{PSC}$
Capacitance Probe	Soil-Water Content (θ_v)	$0 \leq \theta_v \leq \theta_s$
Heat Dissipation Unit	Soil-Water Pressure (ψ)	$-100\ m \leq \psi \leq -1\ m$
Heat Dissipation Unit	Soil Temperature (T_{soil})	$0°C \leq T_{soil} \leq 30°C$
Drain Gauge	Annual Soil-Water Drainage (D)	$0 \leq D \leq P_{annual}$
Rain Gauge	Precipitation (P)	Annual value is within ±50% HMS measured P
Thermister	Air Temperature (T_{air})	Annual average is within ±5% HMS T_{air}

SDR—standard deviation ratio of neutron count
SC—standard count
PSC—previous standard count
P_{winter}—precipitation from November through March
θ_s—saturated water content

Neutron Moisture Probe

Indicators of neutron-probe performance can be acquired using a standard count analysis. A standard count is to be taken before neutron logging as described in Section 2.1. From this analysis, the ratio of the measured standard deviation to the ideal standard deviation, also called the chi-squared test, is calculated and for a properly functioning probe should be between 0.75 and 1.25. If the ratio consistently falls outside these limits, then the probe may be experiencing problems. In addition, the new standard count should be within the previous standard count ±0.98 times the square-root of the previous standard count. A standard count outside of this range is an indication that the probe may not be functioning correctly.

Appendix A and B of the CPN International users manual (CPN International) and the CHG procedure guide (Ross 2007) provide a list of error messages and their meanings as well as a troubleshooting guide. In addition to the information provided in this document, troubleshooting should include evaluating the post processing of the data to verify that the error does not exist in this step. If problems with the neutron probe are not correctable, another neutron probe may be used.

Capacitance Probe

The capacitance-probe performance can be examined using published information (e.g., from the Hanford vadose zone hydrogeology data package by Last et al. 2006). The saturated moisture content value serves as the upper-boundary indicator for capacitance-probe-measured moisture content. Alternatively, a moisture content of zero is set as the lower boundary indicator for the probe. Measurements of capacitance-probe moisture content that fall outside these established boundaries may be considered suspect. Because of subsurface heterogeneities, property uncertainties, and calibration errors, capacitance-probe performance will be reevaluated after sufficient baseline capacitance probe data are acquired.

If the capacitance-probe measurements do not meet the indicators specified, follow the suggested troubleshooting steps presented in Appendix B to identify the problem. If the problem still cannot be solved, remove the capacitance probe from its access tube and visually inspect the probe for damage and moisture accumulation. Replace sensors on the probe and test, and/or bring the probe in from the field for additional examination and possible repair.

If the above steps do not produce a reasonable result, a new probe can be installed using the existing access tube.

Heat Dissipation Unit

Soil-water pressures over the depth of measurement should not be greater than zero, indicating full saturation. However, there is no minimum for soil-water pressure theoretically. In this monitor plan, the HDU measurement range of soil-water pressure, from -1 m to -100 m, is used as the performance indicators. Because of subsurface heterogeneities and property uncertainties, HDU performance will be reevaluated after sufficient baseline capacitance probe data are acquired.

A 50-year monitoring record of soil temperature (Hoitink et al. 2005) in a bare surfaced gravelly sand soil near the HMS provides a range and of soil temperatures to expect in T tank farm. At the 0.9-m depth, the Hoitink et al. (2005) data show that hourly extremes at this site were a minimum temperature of 0.1 °C and a maximum of 29.6 °C. Given the observed results, soil-temperature measurements at a 1-m depth or deeper should not exceed 30°C and should not be less than 0°C. After baseline HDU data are acquired, this performance indicator may be adjusted based on the HDU measurements. However, depending on the color, the surface barrier may transmit heat into the sub-surface soil that may exceed 30C. So, it is expected that thermal regime under the surface barrier may be quite different than that outside the barrier.

If the HDU soil-water pressure or soil temperature measurements do not meet the indicators specified, follow the suggested troubleshooting steps presented in Appendix B to identify the problem. If the above steps do not produce a functioning probe, the installation of new HDUs may be necessary.

Drain Gauge

In the region without a barrier, drainage should not exceed the annual precipitation for that year, unless there is focused flow to the drain gauge due to either a rapid snowmelt event in winter, or possibly a berm failure at the edge of the poly sheet, potentially causing a surface flood after a torrential rainstorm (extreme event). Both conditions are highly unlikely but rapid snowmelt has caused flooding of tank farm surfaces in the past and this condition needs to be recognized. The lower bound of drainage is zero, which means no flux at all.

If the drain-gauge measurements do not meet the indicators specified, confirm if the output from the drain gauge when receiving a voltage excitation is between an appropriate range and follow the suggested troubleshooting steps presented in Appendix B to identify the problem. If the problem still cannot be solved, apply water to the calibration line to see if a flushing event is observed.

If the above steps do not produce a functioning gauge, a new drain gauge may need to be installed.

Precipitation and Air Temperature

Performance bounds for the rain-gauge and air-temperature sensors are set relative to those at the HMS. For calendar year 2004, the most recent year that Hanford climate data are documented, annual precipitation and annual average temperature measured at the 200W monitoring station varied -35.3% and -1.3%, respectively, from those measured at the HMS (Hoitink et al. 2005). Using this information, the annual precipitation data measured at T tank farm should not vary more than ±50% of the HMS precipitation. Likewise, the T tank farm annual average air-temperature data should not vary greater than ±5% of the HMS-measured annual average temperature.

If the rain-gauge or air-temperature measurements do not meet the indicators specified, follow the suggested troubleshooting steps presented in Appendix B to identify the problem. If the problem of the rain gauge still cannot be solved, apply water to the rain gauge to see if a tipping event is observed.

If the above steps do not produce a functioning gauge or thermister, the instrument may be removed and sent to the manufacturer for repair, or a new instrument may need to be installed.

6.3.2 Vadose Zone Response Indicators

Vadose zone response will be monitored by examining systematic changes of subsurface conditions over time as represented by time-history trends at the monitoring locations. The trends in subsurface conditions beneath the interim surface barrier will be used to help answer whether the surface barrier significantly and adequately reduces the downward flux of soil water relative to background conditions. The monitoring plan calls for the direct measurement of downward soil-water flux using drain gauges and indirect measurements using soil-water content and soil-water pressure data.

The drain gauges at Nests A and B were installed at the soil surface and measure the drainage at 0.6 m below the soil surface. The time-history trend of soil-water content below the surface barrier will provide additional information about the effectiveness of the surface barrier in reducing soil-water flux. An effective surface barrier will produce, on average, a drying soil profile beneath the surface barrier, representing a decrease in soil-water flux. Decreasing soil-water flux will also be portrayed by decreasing soil-water pressure relative to baseline conditions. However, it is pointed out that, at very shallow depth, the soil can be completely dry in the summer time when the surface barrier will be emplaced. Then, a redistribution of soil water below the surface barrier will occur, and soil moisture will move upward from the wetter soil at deeper depths to the drier soil in shallow depth until a new equilibrium condition is established.

A clear vadose zone response indicator is a near-surface instrument response after precipitation or snow melt events. Adequate surface-barrier performance should result in no observable increases in moisture content, drainage, or soil-water pressure (less negative) immediately after precipitation or snow-melt events. Such instrument responses would indicate percolating water and general surface-barrier failure, provided the instruments are functioning.

A secondary component of surface barrier performance is the potential advective movement and buildup of water vapor immediately beneath the low-permeable surface barrier. Condensation of the water vapor would result in increased soil-water content immediately below the surface barrier. The vaporization-condensation process does not indicate any problem of the surface barrier because there is no net gain or

loss of water mass across the barrier. The seasonal water movement that might observed by the capacitance probe monitoring, will most likely be due to thermally induced vapor and liquid flow as described above and it is expected that this fluctuation will persist for the life of the barrier. The magnitude of the water content changes and the depth of penetration depend on the soil type and initial water content of the soil, but for typical Hanford conditions it should not extend deeper than a few 10s of cm into the subsurface.

7.0 Quality Assurance

To verify the quality of the project, the organization performing the monitoring will be required to have a project management plan (PMP) and a quality assurance plan (QAP). Quality specialists will provide quality assurance support for the project. Project members will be required to follow the PMP and QAP.

8.0 References

Atlantic-Richfield Hanford Company (ARHCO). 1973. *241-T-106 Tank leak investigation*. ARH_2874, Atlantic-Richfield Hanford Company, Richland, WA.

Campbell Scientific, Inc. (CSI). 2002. Rain Gauges Models TE525WS, TE525, TE525MM, (brochure). Logan, UT.

Campbell Scientific, Inc. (CSI). 2004. Model 107 Temperature Probe Instruction Manual.

Campbell Scientific, Inc. (CSI). 2006a. *EnviroSMART Soil Water Content Profile Probes – Instruction Manual*. Logan, UT.

Campbell Scientific, Inc. (CSI). 2006b. "Soil Volumetric Water Content/Salinity Probes Models EasyAG II and EnviroSMART," (brochure). Logan, UT.

Campbell Scientific, Inc. (CSI). 2006c. "Temperature Probes Models 107 and 108", (brochure). Logan, UT.

CHG. 2006. "Weather and Vadose Zone Monitoring Stations, Electrical Connection Diagram, Rev. 0, Sheet 2, H-14-107368." CH2M HILL Hanford Company, Inc., Richland, Washington.

Decagon Devices, Inc. 2006. Drain Gauge – Gee Passive Capillary Lysimeter User's Manual Version 3.0. Pullman, Washington.

Everett, LG, LG Wilson, and EW Hoylman. 1984. *Vadose Zone Monitoring for Hazardous Waste Sites*. Noyes Data Corporation, Parkridge, New Jersey.

Flint AL, GS Campbell, KM Ellett, and C Calissendorff. 2002. "Calibration and temperature correction of heat dissipation matric potential sensors." *Soil Sci. Soc. Am. J.* 66:1439-1445.

Fredlund DG, F Shuai, and M Feng. 2000. "Use of a new thermal conductivity sensor for laboratory suction measurement." pp. 275-280. In: *Unsaturated soil for Asia.* Rahardjo et al. (ed.). *Proc. of the Asian Conf. on Unsaturated Soils Unsat-Asia 2000*. Singapore.

Gee GW, AL Ward, TG Caldwell, and JC Ritter. 2002. "A vadose zone water fluxmeter with divergence control." *Water Resour. Res.* 38:10.1029.

Hoitink DJ, KW Burk, JV Ramsdell Jr, WJ Shaw. 2005. *Hanford Site Climatological Summary 2004 with Historical Data*. PNNL-15160. Pacific Northwest National Laboratory, Richland, Washington.

International Atomic Energy Agency (IAEA). 1970. Neutron Moisture Gauges. Tech. Rep. Ser. No. 112, Vienna, Austria.

Khaleel R, FJ Anderson, MP Connelly, TE Jones, FM Mann, DA Myers, and MI Wood. 2004. *Modeling data package for WMAs T and TX-TY Field Investigation report*. RPP-17393 Rev. 0, CH2MHiLL Hanford Group, Inc., Richland, WA.

Myers DA. 2005. *Field Investigation Report for Waste Management Areas*. RPR-23752, CH2M Hill Hanford Group, Richland, WA.

Paltineanu IC, and JL Starr. 1997. "Real-time soil water dynamics using multisensor capacitance probes: laboratory calibration." *Soil Sci. Soc. Am. J.* 61:1576-1585.

Reece C. 1996. "Evaluation of a line heat dissipation sensor for measuring soil matric potential." *Soil Sci. Soc. Am. J.* 60:1022-1028.

Ross L. 2007. "Tank Farm Plant Operating Procedure - Operate Model 503DR Hydroprobe Neutron Moisture Detection." TO-320-022, B-8. CH2M Hill Hanford Group, Richland, WA.

Routson RC, WH Price, DJ Brown, and KR Fecht. 1979. *High-level waste leakage from the 241-T-106 tank at Hanford*. RHO-ST-14, Rockwell Hanford Operations, Richland, WA.

Scanlon BR, BJ Andraski, and J Bilskie. 2002. "Miscellaneous methods for measuring matric or water potential." In: *Methods of Soil Analysis Part 4 Physical Methods*. Dane JH and GC Topp (eds.), pp. 643-654. *Soil Science Society of America Inc.* Madison, Wisconsin, USA.

Sentek Pty Ltd. 2001. *Calibration of the Sentek Pty Ltd Soil Moisture Sensors*. Stepney, Australia.

Serne RJ, BN Bjornstad, DG Horton, DC Lanigan, HT Schaef, CW Lindenmeier, MJ Lindberg, RE Clayton, VL LeGore, KN Geiszler, SR Baum, MM Valenta, IV Kutnyakov, TS Vickerman, RD Orr, CF Brown. 2004. *Characterization of Vadose Zone Sediments Below the T Tank Farm: Boreholes C4104, C4105, 299-W10-196, and RCRA Borehole 299-W11-39*. PNNL-14849, Pacific Northwest National Laboratory, Richland, Washington.

Shiozawa S and GS Campbell. 1990. "Soil thermal conductivity." *Remote Sens. Rev.* 5:301-310.

Smith-Rose RL. 1933. "The electrical properties of soils for alternating currents at radio frequencies." *Proc. R. Soc. London* 140:359.

Starr JL and IC Paltineanu. 2002. "Capacitance Devices." In: *Methods of soil analysis Part 4 Physical methods*, Dane JH and GC Topp (eds.), pp. 463-475. *Soil Science Society of America, Inc.*, Madison Wisconsin.

U.S. Department of Energy (DOE). 2005. *Hanford Tank Farms Vadose Zone Monitoring Project, Annual Monitoring Report for Fiscal Year 2004*. DOE-EM/GJ777-2004, Grand Junction Office, Grand Junction, CO.

van Bavel, CHM, N Underwood, and RW Swanson. 1956. "Soil moisture measurement by neutron moderation." *Soil Sci.* 82:29-41.

van Genuchten MTh. 1980. "A closed-form equation for predicting the hydraulic conductivity of unsaturated soils." *Soil Science Society of America Journal* 44:892-898.

Ward AL, TC Caldwell, and GW Gee. 2000. *Vadose Zone Transport Field Study: Soil Water Content Distribution by Neutron Moderation*. PNNL-13795, Pacific Northwest National Laboratory, Richland, WA.

White MD, and M Oostrom. 2004. *User's Guide of STOMP – Subsurface Transport Over Multiple Phases*, Version 3.1. PNNL-14478, Pacific Northwest National Laboratory, Richland, Washington.

Zhang ZF, and JM Keller. 2006. *T Tank Farm Interim Cover Test - Design Plan*. PNNL-15913 Rev. 0, Pacific Northwest National Laboratory, Richland, Washington.

Appendix A

Heat Dissipation Unit Probe Normalization and Calibration Procedures

Appendix A: Heat Dissipation Unit Probe Normalization and Calibration Procedures

This procedure is adapted from HDU normalization and calibration procedures discussed in Scanlon et al. (2002) and Flint et al. (2002).

Normalization

1. Place oven dried desiccant and one or more HDUs in a sealed container and allow to equilibrate for a minimum of 24 hours. If the HDU ceramic has been previously wetted, the HDU is best dried in an oven not to exceed 60°C.
2. Measure temperature rise a HDU using the same heat source current and heating time to be used for the field measurements. This is the temperature rise for dry ceramic (ΔT_d). Repeat Step 2 for other HDUs.
3. Place one or more HDUs in deaired water and allow to equilibrate for a minimum of 24 hours.
4. Remove a HDU from water and immediately measure HDU temperature rise using the same heat source current and heating time to be used for the field measurements. This is the temperature rise for saturated ceramic (ΔT_w). Repeat Step 4 for other HDUs.

Calibration

1. Wet soil to desired soil water pressure condition. Wet soil by thoroughly mixing soil and added water. The amount of water needed to obtain a specified soil water pressure condition can be approximated with prior knowledge of the soil's soil water characteristics curve and the mass of soil.
2. Obtain a minimum of two tensiometers to provide an independent reading of soil water pressure.
3. Pack wetted soil, HDUs and tensiometers into a bucket of five gallons or larger. A minimum of three HDUs should be used to obtain the calibration.
4. Seal the top of the bucket to reduce evaporative water loss from the soil.
5. Measure HDU temperature rise using the same heat source current and heating time to be used for the field measurements.
6. Measure tensiometer pressure.
7. Once HDU temperature rise and tensiometer pressure measurements stabilize, record tensiometer pressure and HDU temperature rise. This is one calibration point.
8. Repeat steps 1 through 7 with a different soil water content until all desired calibration points are obtained. Obtain a minimum of three calibration points. The calibration points should span the anticipated HDU measurement range in the field.
9. Fit appropriate calibration curve to paired soil water pressure and normalized HDU data points.

References

Flint AL, GS Campbell, KM Ellett, and C Calissendorff. 2002. Calibration and temperature correction of heat dissipation matric potential sensors. Soil Sci. Soc. Am. J. 66:1439-1445.

Scanlon BR, BJ Andraski, and J Bilskie. 2002. Miscellaneous methods for measuring matric or water potential. In Dane JH and GC Topp (eds.) *Methods of Soil Analysis Part 4 Physical Methods*, pp643-654. Soil Science Society of America Inc. Madison, Wisconsin, USA.

Appendix B

Suggested Troubleshooting Procedures

Appendix B: Suggested Troubleshooting Procedures

If measurements from an instrument or a sensor do not meet the indicators specified, the following suggested troubleshooting steps should be taken in the order presented. Note that troubleshooting Steps 1 through 3 are performed outside the tank farm. If Steps 1 through 3 do not resolve the issue, entrance into the tank farm is required for further troubleshooting.

1. Review the post processing procedure to verify that the error does not reside in this step.
2. Check the battery voltage data for power supply.
3. Check the datalogger program for potential program error.
4. Manually download the data from the datalogger to confirm that the data error is not created during remote data transmittal to the server.
5. Check the datalogger ports to confirm that they are functioning.
6. Inspect the wiring and connections at the datalogger for disconnections or wiring wear.
7. Inspect the wiring coming out of the top of the probe for disconnection or wiring wear.
8. Test the wiring from the probe to the datalogger for continuity.

Distribution List

No. of
Copies

ONSITE

10	CH2M-HILL Group, Inc.	
	C.D. Wittreich(5)	E6-35
	J.G. Field	E6-35
	F.M. Mann	E6-35
	D.A. Myers	E6-35
	N.L. Peters	E6-35
	H.A. Sydnor	E6-35
1	Energy Solutions	
	K.D. Kent	H1-11
10	Pacific Northwest National Laboratory	
	Z.F. Zhang (3)	K9-36
	M.J. Fayer	K9-36
	G.W. Gee	K9-36
	J.M. Keller	K9-36
	R.R. Kirkham	K9-36
	C.E. Strickland	K9-36
	A.L Ward	K9-36
	Information Release (2)	K1-06